

Polymer Chemistry

Accepted Manuscript



This is an *Accepted Manuscript*, which has been through the Royal Society of Chemistry peer review process and has been accepted for publication.

Accepted Manuscripts are published online shortly after acceptance, before technical editing, formatting and proof reading. Using this free service, authors can make their results available to the community, in citable form, before we publish the edited article. We will replace this *Accepted Manuscript* with the edited and formatted *Advance Article* as soon as it is available.

You can find more information about *Accepted Manuscripts* in the [Information for Authors](#).

Please note that technical editing may introduce minor changes to the text and/or graphics, which may alter content. The journal's standard [Terms & Conditions](#) and the [Ethical guidelines](#) still apply. In no event shall the Royal Society of Chemistry be held responsible for any errors or omissions in this *Accepted Manuscript* or any consequences arising from the use of any information it contains.

ATRP-based Polymers with Modular Ligation Points under Thermal and Thermomechanical Stress

Ozcan Altintas,^{1,2,3} Thomas Josse,⁴ Mahdi Abbasi,² Julien De Winter,⁴ Vanessa Trouillet,⁵ Pascal Gerbaux,⁴ Manfred Wilhelm^{2*} and Christopher Barner-Kowollik^{1,3*}

¹Preparative Macromolecular Chemistry, Institut für Technische Chemie und Polymerchemie, Karlsruhe Institute of Technology (KIT), Engesserstr. 18, 76128 Karlsruhe, Germany.

²Polymeric Materials, Institut für Technische Chemie und Polymerchemie, Karlsruhe Institute of Technology (KIT), Engesserstr. 18, 76128 Karlsruhe, Germany.

³Institut für Biologische Grenzflächen, Karlsruhe Institute of Technology (KIT), Hermann-von-Helmholtz Platz 1, 76344 Eggenstein-Leopoldshafen, Germany.

⁴Interdisciplinary Center for Mass Spectrometry (CISMa), Organic Synthesis and Mass Spectrometry Laboratory, University of Mons, 23 Place du Parc, B-7000 Mons, Belgium.

⁵Institute for Applied Materials (IAM) and Karlsruhe Nano Micro Facility (KNMF), Karlsruhe Institute of Technology (KIT), Hermann-von-Helmholtz-Platz 1, 76344 Eggenstein-Leopoldshafen, Germany.

ABSTRACT

Linear polystyrenes carrying a mid-chain triazole, ester as well as terminal secondary bromine functionalities were synthesized via activators regenerated by electron transfer (ARGET) atom transfer radical polymerization (ATRP) using a bifunctional triazole containing initiator ($3.8 \text{ kDa} \leq M_{n,SEC} \leq 125 \text{ kDa}$, $1.08 \leq D \leq 1.19$) with the aim of understanding their behavior under thermal and thermomechanical stress. As reference materials – isolating the influence of the individual functional groups – three polystyrene homopolymers carrying an ω -bromine chain-end functionality, α,ω -ester-bromine functionalities as well as α,ω -dibromine/mid-chain ester functionalities ($2 \text{ kDa} \leq M_{n,SEC} \leq 39 \text{ kDa}$, $1.06 \leq D \leq 1.08$) were prepared via ARGET ATRP. Furthermore, a well-defined triazole mid-chain functionalized block homopolymer, *i.e.* polystyrene-*b*-polystyrene (PS-*b*-PS, $M_{n,SEC} = 4.4 \text{ kDa}$, $D = 1.08$) was synthesized *via* a combination of ARGET ATRP and copper (I)-catalyzed azide-alkyne cycloaddition (CuAAC) as a reference material. Reference polymers without bromine and with ester/triazole functionalities

were additionally investigated. Thermomechanical stress was applied to the polymers via small scale extrusion as well as a rheological assessment ($G'_{(t)}$, $G''_{(t)}$) under processing conditions. The thermally challenged polymers were analyzed via size-exclusion chromatography (SEC), matrix-assisted laser desorption/ionization time-of-flight mass spectrometry (MALDI-ToF-MS), proton nuclear magnetic resonance (^1H NMR) as well as X-ray photoelectron spectroscopy (XPS) to arrive at a detailed image of the degradation susceptibility of the individual functional groups especially esters, bromines and triazole functions. The findings indicate an enhanced degradation of ATRP polymers via an accelerated ester cleavage due to HBr release at high temperatures accompanied by a concomitant molecular weight increase due to the formation of triazolium salts via the reaction of triazole units with bromine terminal chain ends.

INTRODUCTION

The copper-catalyzed azide and alkyne cycloaddition (CuAAC) – a reaction often fulfilling the *click* criteria – introduced by Sharpless and coworkers in 2001,¹ is a selective and orthogonal reaction that can function under mild conditions with high yields, simple recovery of the product, compatibility to a wide range of solvents, often excellent functional group tolerance and no side products.²⁻³ The application of the CuAAC reaction in conjunction with living radical polymerization (LRP)⁴ has contributed to the fast development of precision materials⁵ and polymer architectures such as functional polymers,⁶ block copolymers,⁷ complex macromolecular structures,⁸ networks⁹ and dendrimers.¹⁰

The most commonly employed LRP techniques include atom transfer radical polymerization (ATRP),¹¹ reversible addition-fragmentation transfer (RAFT) polymerization,¹² and nitroxide-mediated radical polymerization (NMP).¹³ Especially atom transfer radical

polymerization (ATRP) is highly versatile and efficient LRP technique allowing for the generation of polymers with pre-determined molecular weight, narrow molecular weight distribution, chain-end functionality, adjustable architecture and composition. Activators regenerated by electron transfer (ARGET) ATRP can be utilized to generate block copolymers using a large excess of reducing agent to obtain the activator from the deactivator, allowing transition metal concentrations at low ppm levels without loss of control.¹⁴ This advantage could have profound industrial implications for the synthesis of well-defined polymeric materials.

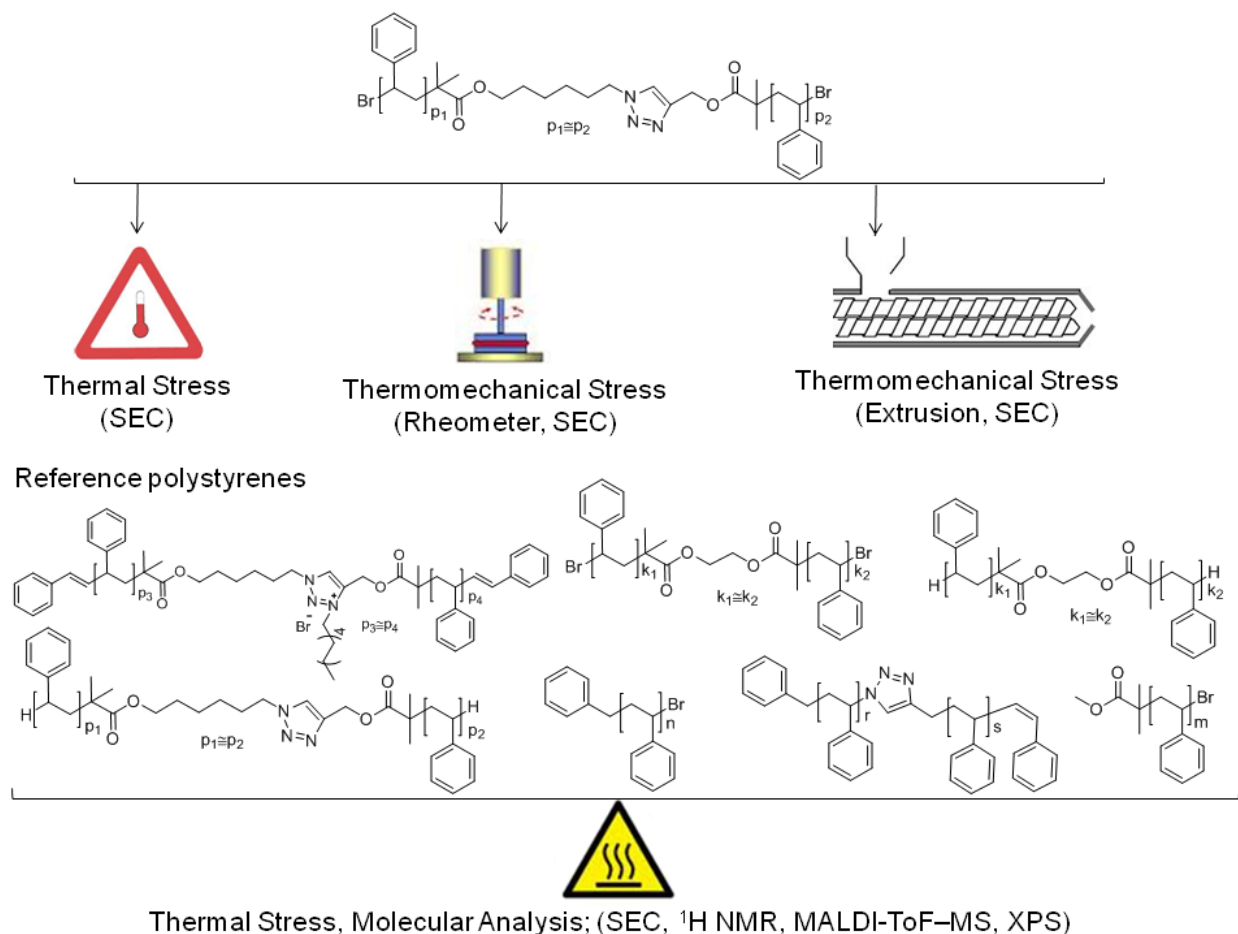
The arguably most prepared polymer architectures are linear, branched and cross-linked structures. A detailed understanding of the molecular changes occurring within precision tailored polymeric materials under the effects of combined thermal and mechanical stress is a key requirement for their processing of thermoplasts *via* e.g. extrusion and injection molding and techniques alternative high temperature shape giving processes.

Linear or star block copolymers with various compositions have been synthesized via one of three methodologies, *i.e.* core-first, arm-first and chain extension.¹⁵ These synthetic methods differ from each other based on the sequence employed for the formation of the core and the arms. In the core-first approach, multifunctional initiators are used to grow arms via living polymerization techniques. Significant research efforts have been made to achieve block copolymers with complex architectures via the core-first or arm-first approach and combinations of LRP and CuAAC.¹⁶ However, detailed knowledge regarding the thermal and thermomechanical stability of the resulting polymeric materials under industrially relevant processing conditions (e.g. melt extrusion) is critically required. We have commenced a research program into the stability of initially linear and star-shaped RAFT-based polystyrene melts featuring mid-chain trithiocarbonate functions (*i.e.* a Z-group design) under thermal and

thermomechanical stress. Our activities are designed to develop a detailed understanding of the mechanistic changes occurring during thermomechanical and thermal stress of precision polymeric materials while concomitantly understanding changes in their rheological and processing properties under stress.^{17,18} To the best of our knowledge, there exists no previous study assessing the stability of ATRP-based polymers under thermal stress and thermomechanical stress. In addition, most commercially available ATRP initiators leading to block copolymers and multi-arm star polymers incorporate ester functionalities, which are one of the groups at the center of our current investigation. Thus, any processing of polymers based on ATRP initiators containing ester or triazole functions which connect the polymer arms is covered by the results of our current investigation.

In the present study, we thus investigate the stability of linear polystyrene melts with a diblock homopolymer topology that carry mid-chain triazole and ester as well as bromine chain end functionalities under thermal and thermomechanical stress. The approach taken in the current study entails the detailed analysis of polymer structures of decreasing macromolecular complexity in order to isolate the effect of thermal stress on the individual functional entities. Initially, linear polystyrenes with specific functional groups (refer to Scheme 1 for an overview) were synthesized via ARGET ATRP using a bifunctional triazole and ester containing initiator ($3.8 \text{ kDa} \leq M_{n,SEC} \leq 125 \text{ kDa}$, $1.07 \leq D \leq 1.19$). In addition – enabling the noted isolation of effects – polystyrenes of low molecular weight featuring an ω -bromine chain-end functionality, α,ω -ester-bromine functionalities, α,ω -dibromine / mid-chain ester functionalities as well as α,ω -dibromine / mid-chain ester and triazole functionalities were prepared. Finally, a well-defined triazole mid-chain functionalized polystyrene (with no other functionalities) was additionally synthesized *via* a combination of ARGET ATRP and CuAAC. To eliminate the effect of the

bromine end-group functionalities of the α,ω -dibromine / mid-chain ester functional as well as α,ω -dibromine / mid-chain ester and triazole functional polystyrenes, the bromine termini are readily transformed into hydrogen end groups in the presence of tributyltin hydride.



Scheme 1. Experimental approach for understanding the behavior of modular ATRP polymers carrying various functional groups specially ester, triazole and bromine under mechanical and thermal stress.

The thermal and thermomechanical stability of the functional polystyrenes was studied at elevated temperatures (e.g. 180 or 200 °C) under an inert atmosphere. Low molecular weight variants of the polymers were subjected to identical thermal conditions as applied during thermal

stress as well as extrusion and rheometry of their long chain equivalents prior to MALDI-ToF analysis to explore the mechanism of degradation associated with variable functional groups.

In a subsequent step, the (modular) ATRP polymers were investigated via rheological experiments ($G'_{(t)}$, $G''_{(t)}$) to implement a link between the time dependent SEC data and potential processing conditions. Furthermore, rheological assessments are highly sensitive and feature – in contrast to the SEC experiments – a high time resolution ($\Delta t < 1$ min.) to monitor molecular changes within the polymer structure. Weight-average molecular weight dependency of zero shear viscosity, $\eta_0 \sim M_w^{3,4}$, as shown by the reptation theory for linear homopolymers¹⁹⁻²² thus providing a fine sensor with a fast time resolution for possible polymer cleavage reactions.

EXPERIMENTAL SECTION

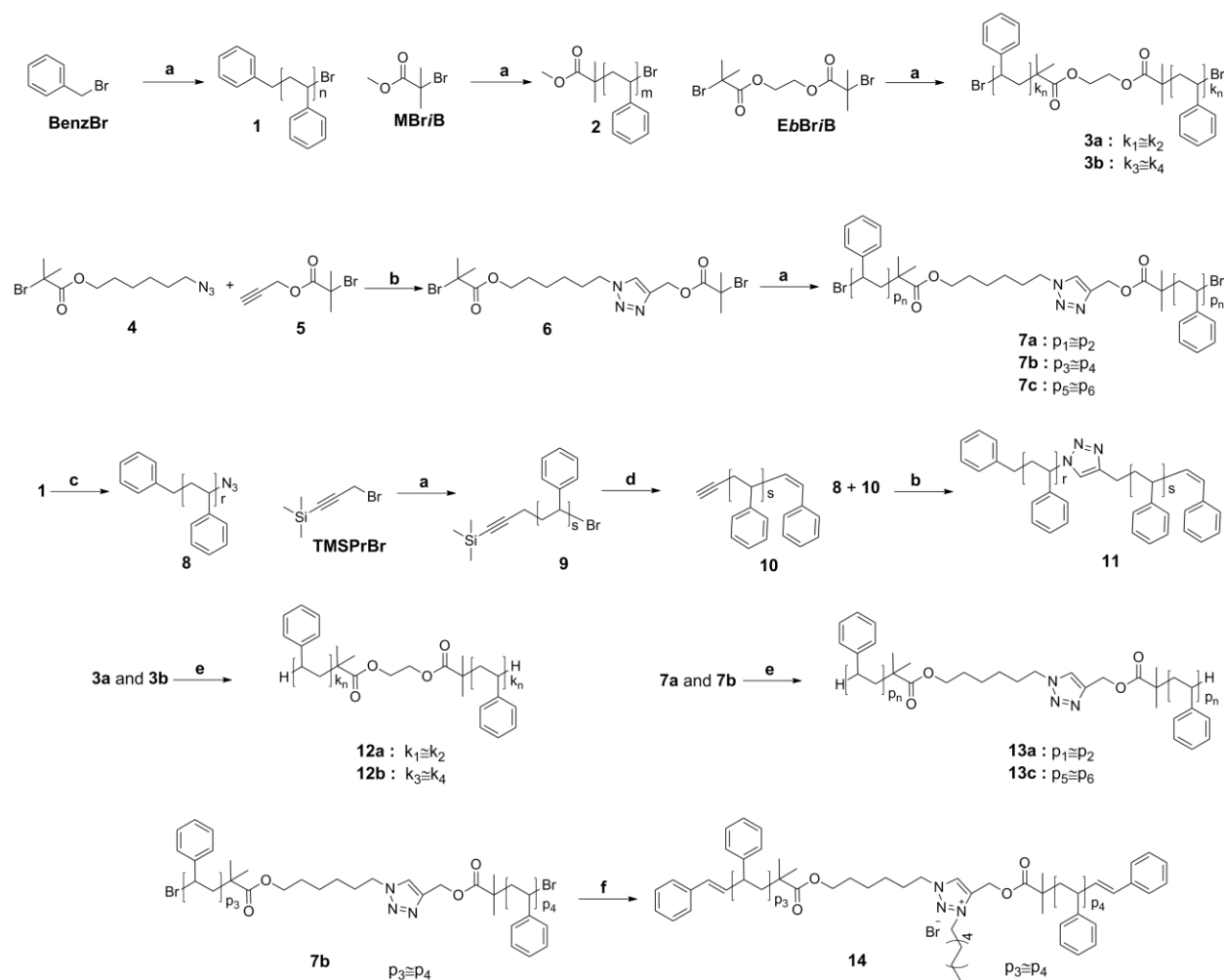
Synthesis

6-Azidohexyl 2-bromo-2-methylpropanoate (**4**) and prop-2-yn-1-yl 2-bromo-2-methylpropanoate (**5**) were synthesized according to literature procedures.^{23,24} The characterization data of all prepared polymers can be found in Figure 1 and 2 (full molecular weight distribution) as well as in Tables 1a and 1b (numeric data). The Supporting Information contains further details regarding the employed materials, synthetic procedures, instrumentation, as well as additional detailed characterization. The interested reader is kindly referred to the Supporting Information section for in-depth synthetic information as well as characterization.

RESULTS AND DISCUSSION

ATRP has emerged as one of the most powerful synthetic techniques in polymer chemistry, being tolerant towards many solvents, functional groups and impurities often

encountered in industrial systems.²⁵ Several variations of the ATRP technique have been developed to overcome the relatively large amounts of copper catalyst present in a classic ATRP system. The new ATRP initiation techniques such as ARGET use very small amounts of catalyst, which could have a beneficial impact on the application of ATRP in industry. In particular, the combination of ATRP and CuAAC allows for the synthesis of well-defined polymers with precise functionality. However, it is mandatory to understand the stability as well as reactivity of ATRP-made polymers, the stability of the functional groups typically present in the initial ATRP initiators (ester linkages) and the triazole unit generated by CuAAC under both thermal and mechanical stress to eventually allow ATRP and CuAAC based polymers to be processed.



Scheme 2. Synthetic strategy for the preparation of the different linear polystyrenes employed in the present study carrying selected functionalities in a mid-chain and terminal position. a) styrene, CuBr₂, Me₆TREN, Sn(EH)₂, anisole, 90 °C; b) CuSO_x5H₂O, Na ascorbate, DMF, room temperature; c) NaN₃, DMF, room temperature; d) TBAF, THF, room temperature; e) tributyltin hydride (TBTH), toluene, 85 °C, 4.5 h; f) decyl bromide, DMF, 100 °C, 16 h.

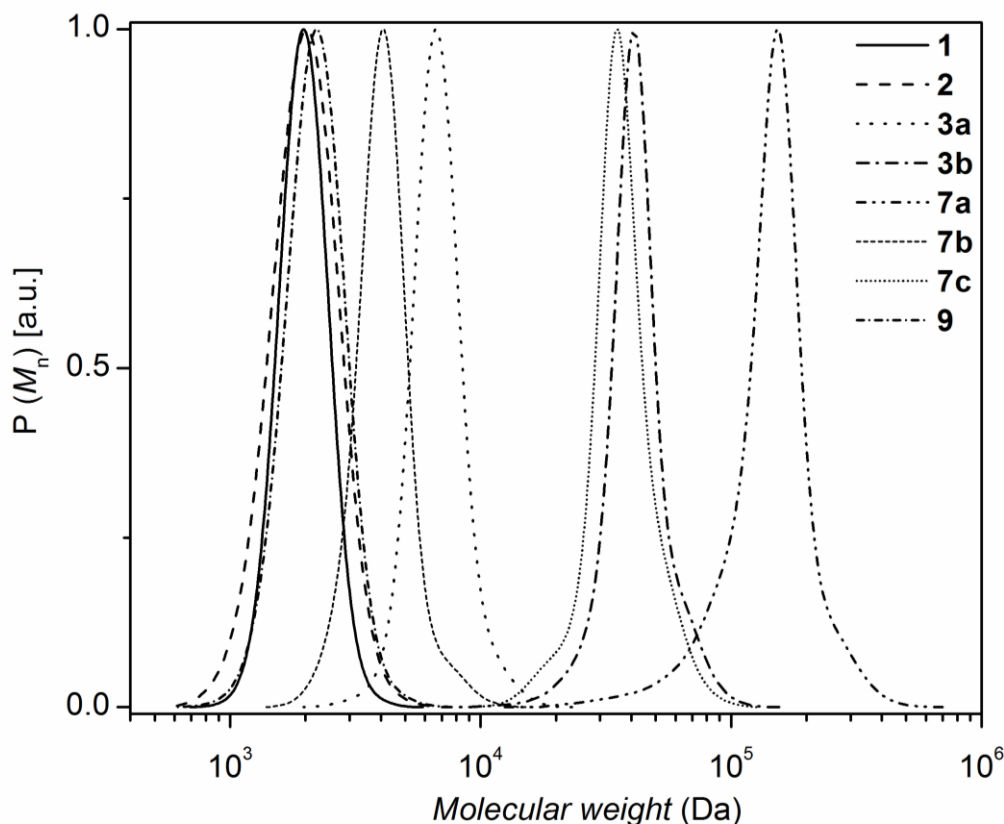


Figure 1. SEC traces of the synthesized functional linear polystyrenes employed in the stability assessments, rheometry and extrusion experiment prior to thermal/mechanical stress: **1** ($M_{n,SEC} = 2$ kDa, $D = 1.06$), **2** ($M_{n,SEC} = 2$ kDa, $D = 1.10$), **3a** ($M_{n,SEC} = 6.5$ kDa, $D = 1.06$), **3b** ($M_{n,SEC} = 39$ kDa, $D = 1.08$), **7a** ($M_{n,SEC} = 124.7$ kDa, $D = 1.19$), **7b** ($M_{n,SEC} = 3.8$ kDa, $D = 1.07$), **7c** ($M_{n,SEC} = 33.8$ kDa, $D = 1.09$), and **9** ($M_{n,SEC} = 2.1$ kDa, $D = 1.08$). The molecular weight distributions of the polymers **8**, **10** and **11** are depicted in Figure 2.

Styrene was polymerized under ARGET ATRP conditions in anisole at 90 °C using the CuBr₂/Me₆TREN catalytic system and Sn(EH)₂ as a reducing agent. Linear mid-chain triazole functional polystyrenes were obtained using **6** as an initiator via the core-first approach to ensure that each chain contains triazole functionality. Commercially available benzyl bromide (**BenzBr**), methyl 2-bromoisobutyrate (**MBriB**), ethylene bis(2-bromoisobutyrate) (**EbBriB**) and 3-(trimethylsilyl)propargyl bromide (**TMSPrBr**) molecules were employed as initiators for the ARGET ATRP of styrene under the above conditions. First of all, ω-bromine functional polystyrene (**1**) was synthesized to investigate the effect of the bromine atom during thermal stress. Secondly, the stability of ester and bromine functionalities was jointly studied using α,ω-ester-bromine functional polystyrene (**2**). Thirdly, α,ω-dibromine functional and mid-chain ester functional linear polystyrene (**3a** and **3b**) were prepared. Finally, the bromine end-group functionalities of the polystyrenes (**3a** and **3b**) and polystyrenes (**7a** and **7c**) were transformed into hydrogen termini in the presence of tributyltin hydride to obtain the polystyrenes (**12a** and **12b**) as well as polystyrenes (**13a** and **13c**), respectively, allowing for the investigation of the stability of the ester group in the absence of bromine end groups. The polystyrenes were subjected to SEC analysis, indicating monomodal molecular weight distributions with low molar mass dispersities. The resulting molecular weight distributions are depicted in Figure 1 and the associated reaction conditions are collated in Table 1a and 1b. Linear polystyrenes carrying ester and bromine functionalities with low molecular weight were prepared for ¹H NMR and MALDI analyses as reference polymers to understand the cleavage processes on the molecular level.

Table 1a. Reaction conditions employed for the preparation of the initial polymers *via* the ARGET ATRP process as well as associated number-average molecular weights.

Polymer ^a	Monomer	[M ₀]/[I ₀]	Initiator	Reaction time (h)	M _n ^b	Đ ^b
1	Styrene	50	BenzBr	2.5	2 kDa	1.06
2	Styrene	50	MBriB	2.5	2 kDa	1.10
3a	Styrene	50	EbBriB	2.5	6.5 kDa	1.06
3b	Styrene	1000	EbBriB	48	39 kDa	1.08
7a	Styrene	2500	6	64	125 kDa	1.19
7b	Styrene	50	6	2.5	3.8 kDa	1.07
7c	Styrene	1000	6	48	33.7 kDa	1.09
9	Styrene	50	TMSPrBr	2.5	2.1 kDa	1.08

^a [I]₀/[Me₆TREN]₀/[CuBr₂]₀/[Sn(EH)₂]₀ = 1:0.1:0.1:0.5; at 90 °C. ^b Determined via RI detection SEC using linear PS standards.

Table 1b. Polymer intermediates and ligation products as well as dehalogenated polymer species

Polymer	M_n^c	\bar{D}
8	2 kDa	1.08
10	2.1 kDa	1.08
11 (8-b-10)	4.3 kDa	1.08
12a	6.1 kDa	1.06
12b	38.5 kDa	1.08
13a	120.1 kDa	1.19
13c	32.5 kDa	1.09
14	4.1 kDa	1.06

^c Determined via RI detection SEC using linear PS standards.

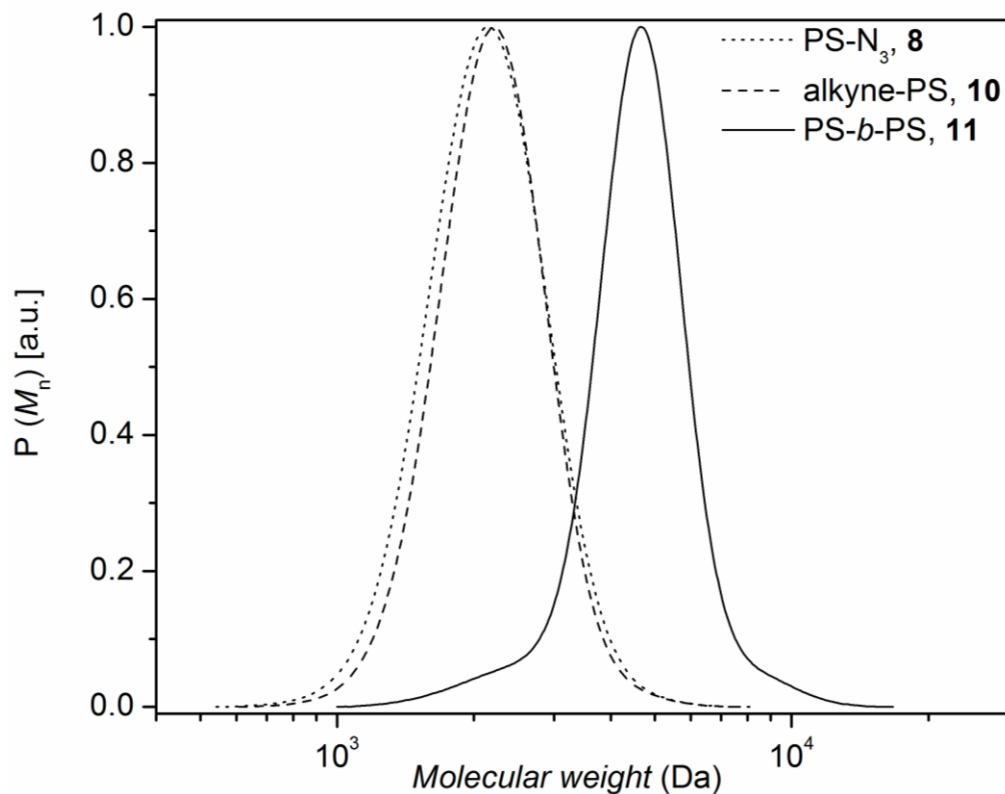


Figure 2. SEC traces of the **8** ($M_{n,SEC} = 2$ kDa, $D = 1.06$) and **10** ($M_{n,SEC} = 2.1$ kDa, $D = 1.08$) building blocks as well as the PS-*b*-PS diblock homopolymer **11** ($M_{n,SEC} = 4.4$ kDa, $D = 1.08$).

The PS-*b*-PS diblock homopolymer was characterized by ^1H NMR, FT-IR spectroscopy and SEC. As illustrated in Figure 2, a complete shift of the distribution towards higher molecular weight was observed indicating the formation of the diblock homopolymer.⁷ The SEC trace of diblock homopolymer (**11**) indicates the presence of very small amounts of precursor polymer, associated with some unavoidable loss of bromine functionality during the ATPR process or non-stoichiometric conditions.

Assessment of Polymer Stability and Cleavage Processes

Having a polymer library with well-defined functional groups at hand which allows for a systematic investigation of the effect that different structural elements have on the degradation

process and the polymer stability, thermal stress experiments were initially carried out. Understanding the degradation of polymer systems in an oxygen rich atmosphere is rather complex.²⁶⁻²⁸ Polymer extrusion of thermoplasts is typically conducted in the melt at elevated temperatures (e.g. 200 °C) and pressures (e.g. 300 bar) and thus the oxygen content is relatively low. The thermal stability of the prepared functional linear polymers has been studied at various temperatures in inert atmospheres to mimic the atmospheric conditions under extrusion as closely as possible. A time resolved SEC analysis allows for estimating the thermal stability of linear polystyrenes with several functionalities as a function of time, yet with a limited time resolution.

The assessment of the stability of the various macromolecular species is commenced with the most complex system, i.e. polystyrene **7a** which features (i) a triazole functionality in mid-chain position, (ii) two carboxylic ester groups on either side of the triazole ring and next to the styryl chains and (iii) a Br-terminus on either end. The cleavage kinetics of the polystyrene **7a** were investigated under isothermal conditions in the melt at different temperatures for pre-set time intervals. For this purpose, the number-average molecular weights, M_n , of the polystyrene **7a** were determined via SEC, indicating that the thermal degradation becomes prominent after 1 h at 180 °C and 200 °C. The change in the molecular weight distribution as a function of time is depicted in Figure 3 and in Figure S5 (refer to the SI section) for degradation at 180 °C and 200 °C for polystyrene **7a**, respectively, indicating an increasing polydispersity index (\mathcal{D}) with time, congruent with the formation of higher molecular weight species as well as lower molecular weight species. Subsequently, the degradation products originating from the polymer were systematically investigated via SEC, ¹H NMR and MALDI-MS analyses in comparison to the reference polymers (**1**, **2**, **3a**, **3b**, **11**, **12a**, **12b**, **13a** and **13c**).

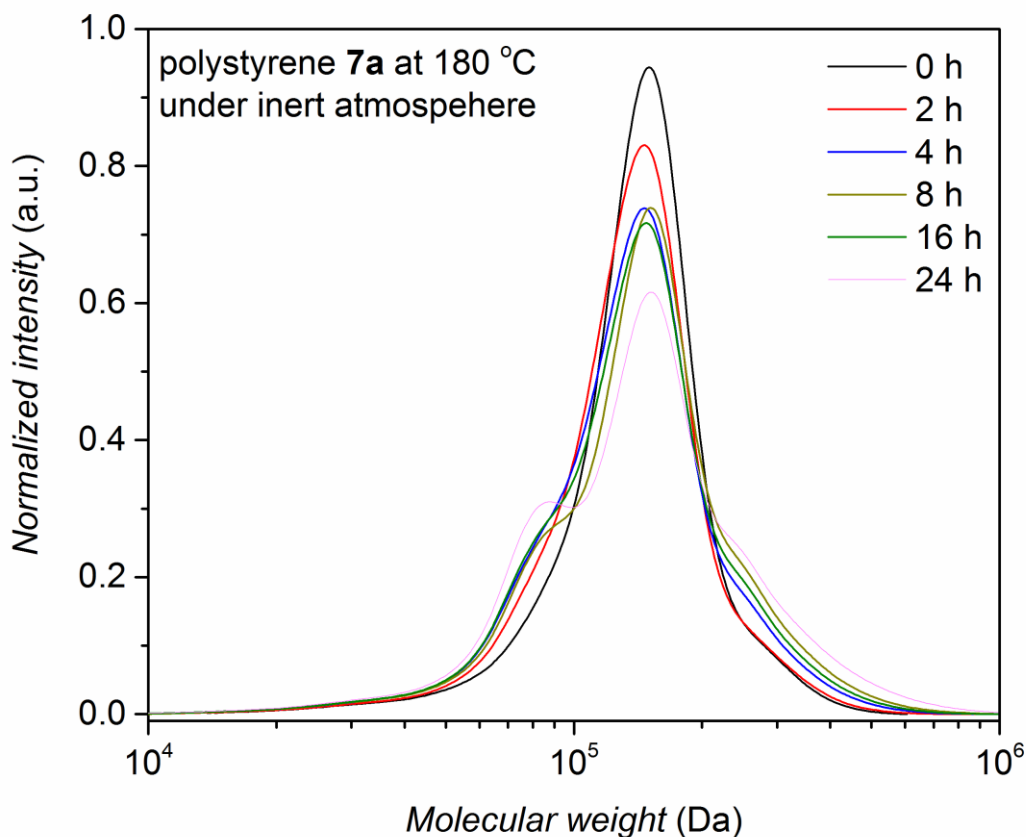


Figure 3. SEC traces of the polystyrene **7a** after thermal treatment at 180 °C in an argon atmosphere as a function of time; 0 h ($M_n = 119.2$ kDa, $D = 1.19$), 2 h ($M_n = 112.6$ kDa, $D = 1.25$), 4 h ($M_n = 109.2$ kDa, $D = 1.32$), 8 h ($M_n = 109$ kDa, $D = 1.35$), 16 h ($M_n = 113.5$ kDa, $D = 1.36$), 24 h ($M_n = 108.4$ kDa, $D = 1.48$). All peaks are normalized to total peak area.

In order to understand the (apparent) complex degradation behaviour of polystyrene **7a** under thermal stress and to isolate the contributions of the individual structural elements to the degradation process, the effect of the secondary alkyl halide and ester functionality at the chain-end position was initially investigated. The polystyrenes **1** (ω -bromine functional) and **2** (α,ω -ester-bromine functional) have been kept at 200 °C in an argon atmosphere for 24 h before SEC

analysis (refer to Figure S6 in the SI section). For the both polymers, no reduction in molecular weight was observed. In addition to SEC analysis, the thermally treated polystyrenes **1** and **2** were analyzed by ^1H NMR and MALDI-MS. The ^1H NMR spectra of polystyrenes **1** and **2** recorded after thermal treatment indicate that the bromine atoms were eliminated from the polystyrene structure generating unsaturated species as well as no effect on the stability of the polystyrene backbone (see Figure S7 and S8 in the SI section).

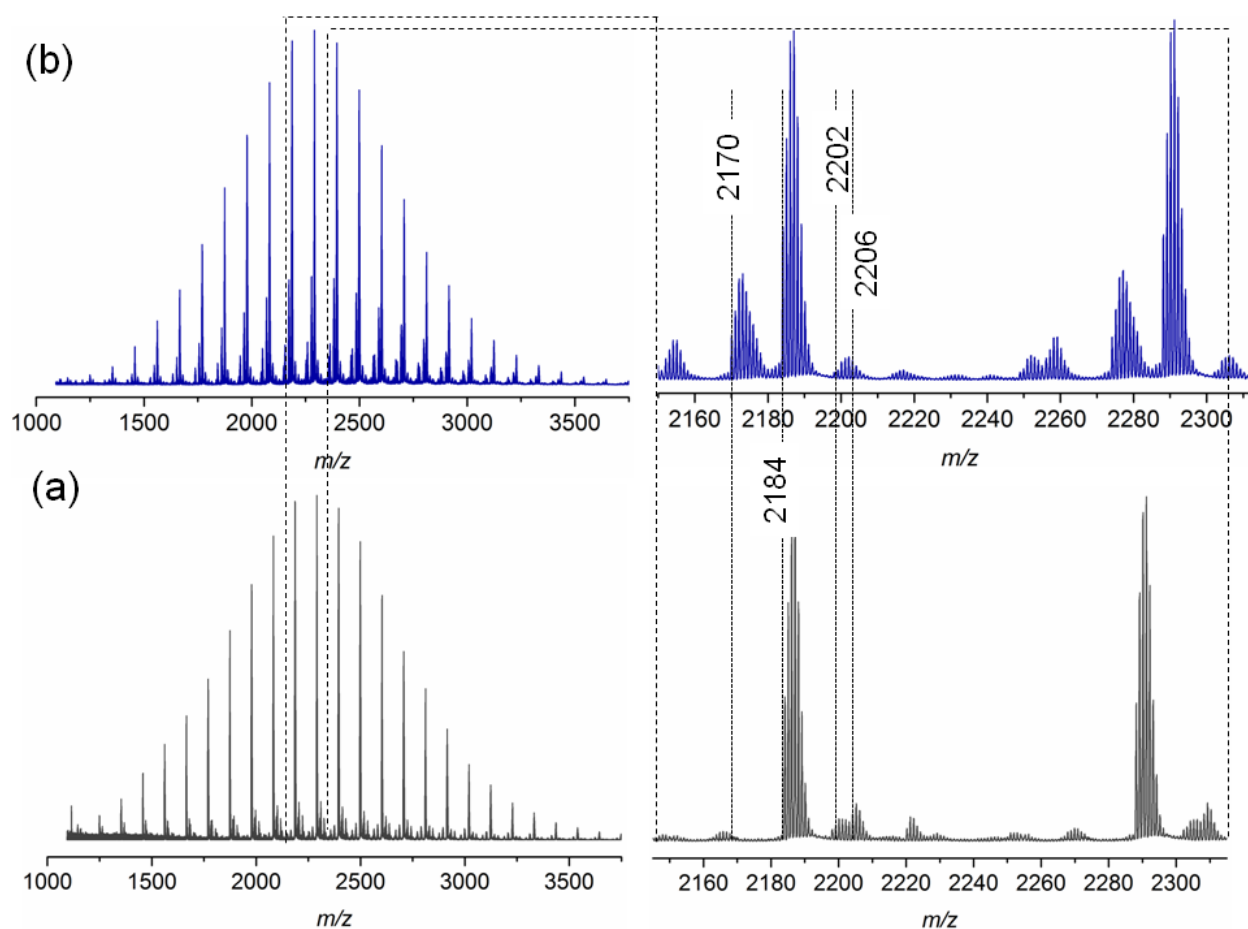
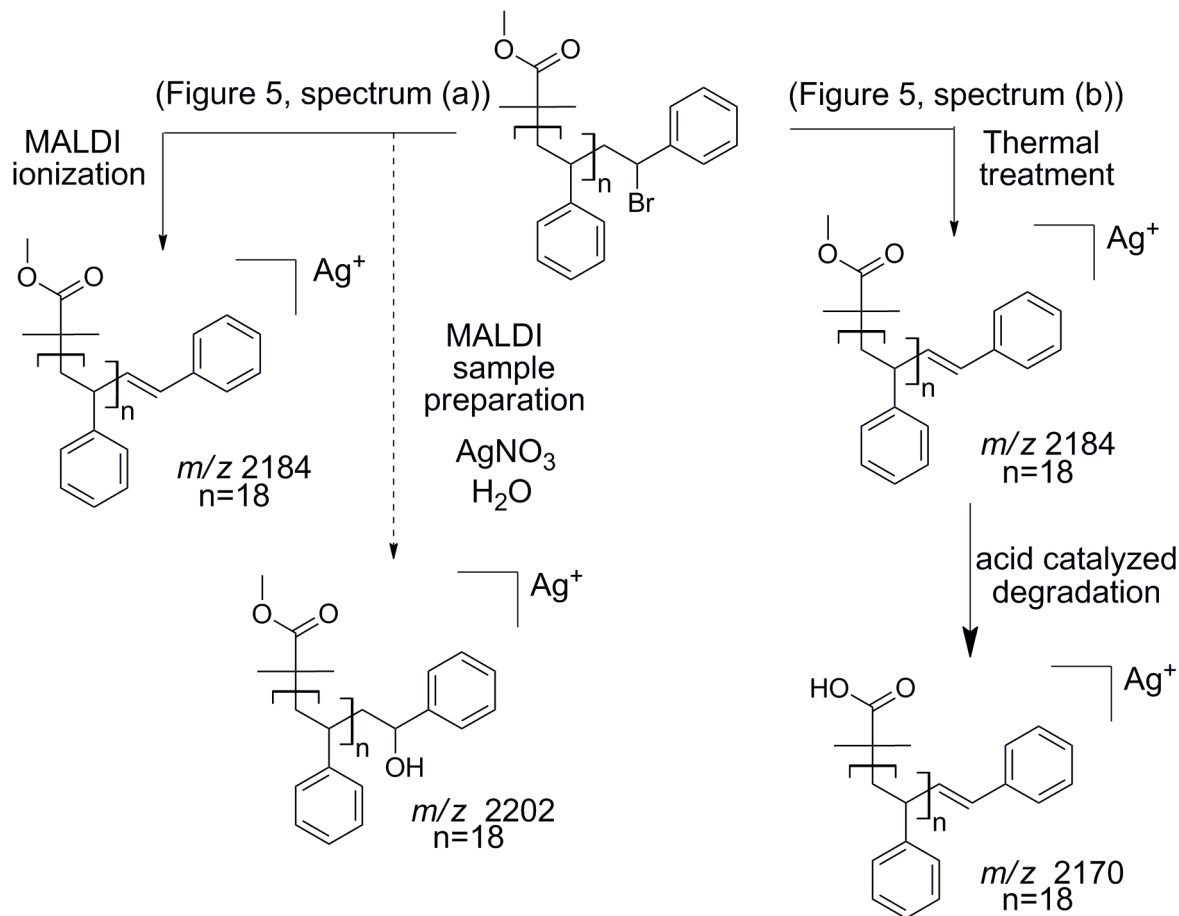


Figure 4. MALDI-MS spectra of ester and bromine functionalized polystyrene **2** before (a) and after (b) thermal treatment at 200 °C for 24 h in an argon atmosphere

In agreement with a recent report of Ladaviere *et al.*,²⁹ bromine terminated polystyrene is subject to HBr elimination during the MALDI ionization processes, leading to unsaturated species. In addition, Ladaviere *et al.* have demonstrated the possibility to substitute the halide atom by a hydroxide moiety in the presence of water traces during the sample preparation. Further, it is important to note that this substitution is promoted by the presence of silver ions, usually used as cationizing agent for the MALDI-MS analysis of polystyrene. Therefore, if only signals characterized by the HBr elimination are observed only in the mass spectrum, bromine elimination occurred both prior to MALDI sample preparation and during analysis. In contrast, the presence of a distribution at 18 mass units higher relative to the unsaturated species confirms the presence of the halide atom at the moment of MALDI sample preparation.



Scheme 3. Description of the processes involved following the MALDI of polymer **2** (a) before and (b) after thermal treatment (200 °C, 24 h).

The mass spectra for polystyrenes **1** and **2** before thermal treatment are presented in Figure S9a and Figure 4a, respectively. The main distribution is attributed to the unsaturated species in both cases. The observation of small signals at 18 mass units higher, i.e. m/z 2296 and 2202 (for clarity, the most intense signal (m/z 2206) of this isotopic distribution is also assigned in the MS spectra) respectively, confirms the presence of the halide before MALDI analysis (refer to Scheme 3 and Scheme S1 for mechanistic details). For polystyrene **1** and **2** after thermal treatment (Figure S9b and Figure 4b), the recorded mass spectra present also as main distribution the unsaturated species, however the signals at 18 mass unit higher are not present anymore, confirming that the HBr elimination has taken place before the ionization processes as already attested by ^1H NMR (see Figures S7 and S8). Moreover, for polystyrene **2**, an additional species appears (refer to Figure 4b) at 14 mass unit lower than the unsaturated polystyrene. This ion series is consistent with the hydrolysis of the methylester moiety under thermal stress.

To explore a possible mechanism of degradation associated with the ester group in polymer **7a**, linear polystyrene with a mid-chain ester and end chain bromine functionality was synthesized via ARGET ATRP utilizing a commercially available bifunctional initiator, affording polystyrene **3a** with a molecular weight of 6100 Da and a polydispersity index of 1.06. Polystyrene **3a** was subjected to identical thermal degradation conditions (i.e. 200 °C for 24 h under inert atmosphere) as polystyrene **1** and **2** prior to SEC, ^1H NMR and MALDI-MS analyses. Inspection of Figure 5 clearly indicates a decrease in the peak-average molecular weight from $M_p = 6600$ Da to $M_p = 3300$ Da for polystyrene **3a** as a consequence of the

appearance of a substantial amount of material with lower molecular weight region. The ^1H NMR spectrum indicates the disappearance of resonances associated with the CH-Br proton and the formation of the unsaturated species as well as a decrease in the intensity of the CH_2 proton resonances adjacent to ester group (see Figure S10 in the SI section). While the SEC analysis suggests that the ester functional polymers are cleaved by mid-chain scission at elevated temperature, a more detailed molecular proof is provided by a mass spectrometric investigation. Based on the MALDI mass spectrum depicted in Figure 6b, the potential mechanism involved during the thermal treatment of polystyrene **3a** is presented in Scheme 4b. In addition to the elimination of both bromines, a 1,5-hydrogen shift involving a six membered ring occurred giving rise to cleavage of the original polystyrene, leading to an carboxylic acid (m/z 2898) end group and a polystyrene with a vinyl function as end-group. However, the latter is not observed by MALDI analysis, yet another ion distribution (m/z 2984) is detected after the thermal treatment.

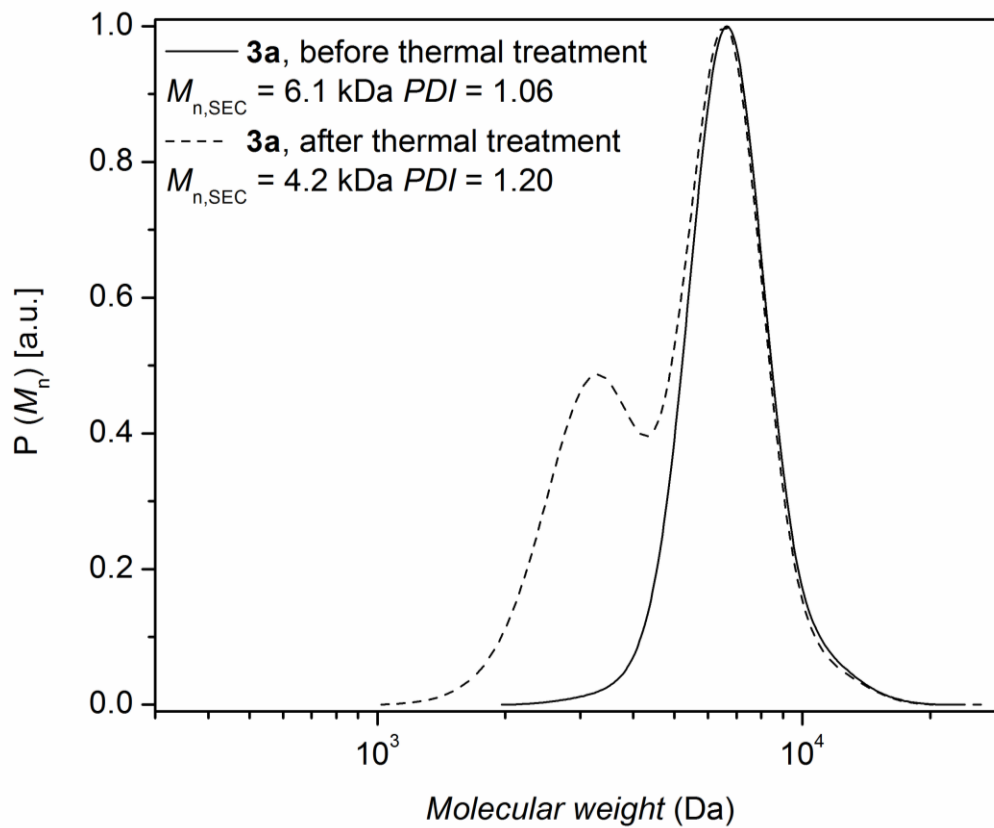


Figure 5. SEC traces of polystyrene **3a** before and after thermal treatment at 200 °C for 24 h in a nitrogen atmosphere.

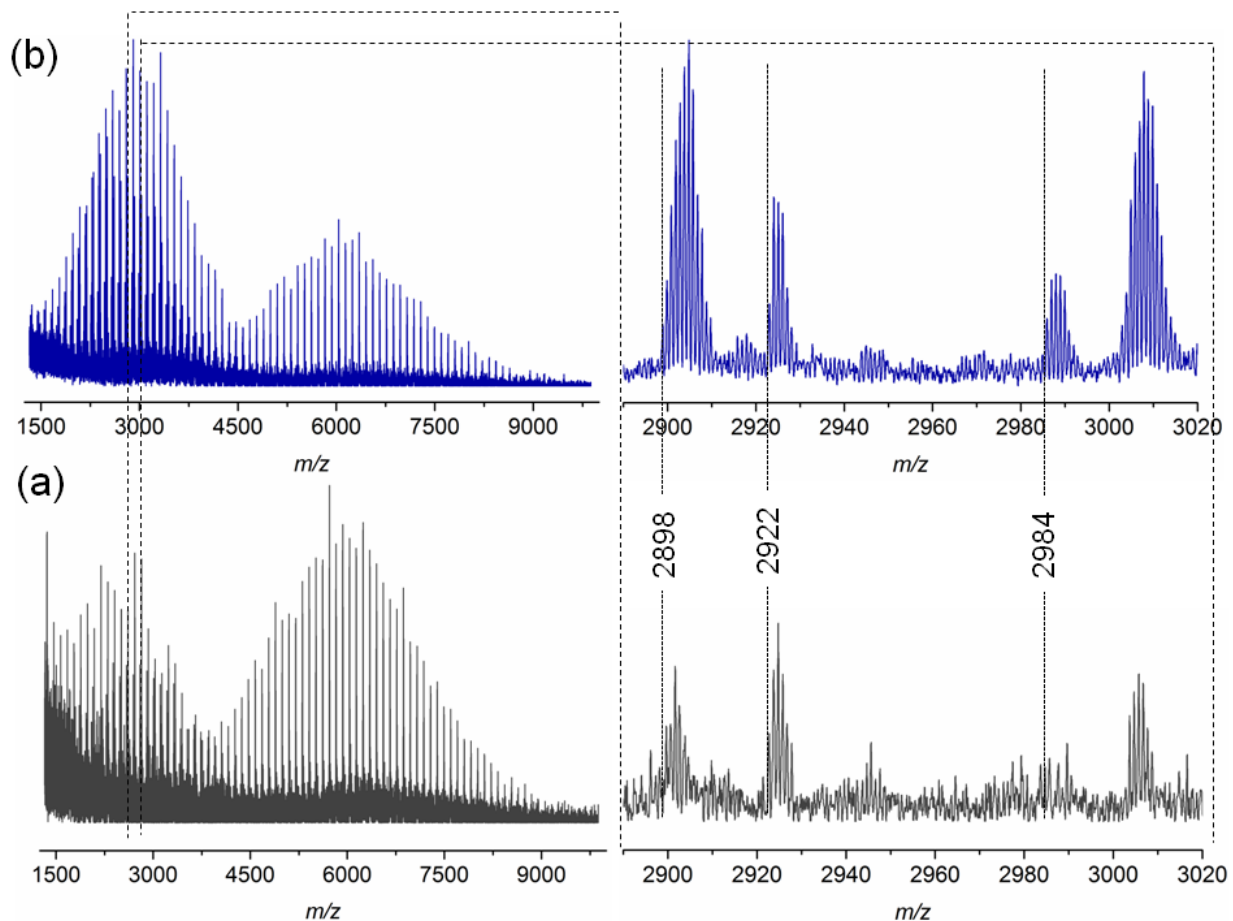
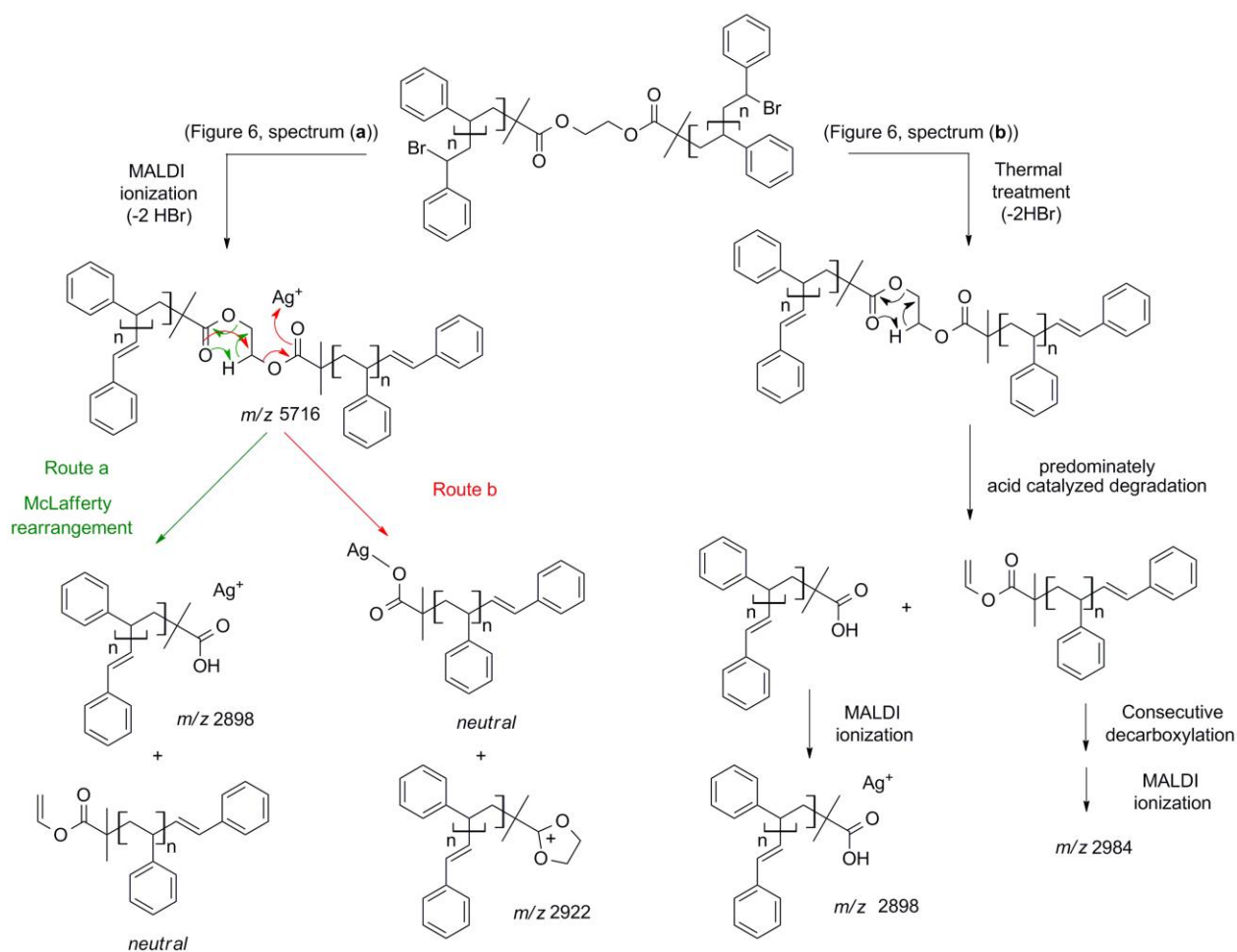


Figure 6. MALDI-MS spectra of polymer **3a** before (a) and after (b) thermal treatment at 200 °C for 24 h in an argon atmosphere.

This new distribution is suspected to originate from a consecutive decarboxylation of the vinyl terminal species (see Scheme 4). The pericyclic rearrangement (1,5-hydrogen shift) can also be induced during the MALDI ionization processes.^{30,31} As a consequence, the MALDI mass spectrum of polystyrene **3a** before thermal treatment (Figure 6a) already shows the presence of a low intensity distribution of polystyrene with carboxylic end-groups (m/z 2898) at lower mass-to-charge ratio (Scheme 4a, route a). The origin of the second ion distribution (m/z 2922) at lower mass range for the untreated polystyrene is explained by a charge localized

fragmentation (Scheme 4a, route b) as reported in the literature.³² Finally, after the thermal treatment of polystyrene **3a**, an inversion of the relative intensities of both distributions is observed. Since all mass spectra have been recorded under exactly the same experimental conditions, the modification of the intensities unambiguously confirms the degradation of the polystyrene as attested by SEC. Moreover, the structures of the low mass-to-charge polystyrene ions are evidence for the ester driven degradation. It was initially assumed that the ester group would be stable at elevated temperature as ester pyrolysis only occurs above 300 °C.³³ A Chugaev-type elimination reaction of aliphatic esters forming acid and olefin usually prevails when a β -hydrogen atom is available in the alcohol part of the ester,³⁴ yet in the presence of bromine functions that lead to the elimination of HBr, an acid catalyzed ester degradation prevails. The newly formed end groups decompose by secondary reactions, e.g. decarboxylation, decarbonylation and anhydrate formation.³⁵



Scheme 4. Description of and mechanistic pathway to the ion structures observed by MALDI-MS analysis (Figure 6) of polystyrene **3a** (a) before and (b) after thermal treatment (200 °C, 24 h).

Subsequently, the stability of the polystyrene featuring a triazole ring as mid-chain function (**11**) was investigated by exposing it to 200 °C for 24 h under an inert atmosphere followed by SEC, ^1H NMR, MALDI-MS and XPS analysis. After applying thermal treatment as noted above, SEC analysis revealed that the molecular weight distributions of polystyrene **11** remains unchanged (Figure S11 in the SI section). The SEC result thus indicates that the triazole mid-chain functional polymer was highly stable under these conditions. ^1H NMR spectrum also

indicates that the resonances associated with CH_2 next to triazole unit are still present after thermal treatment (see Figure S12 in the SI section).

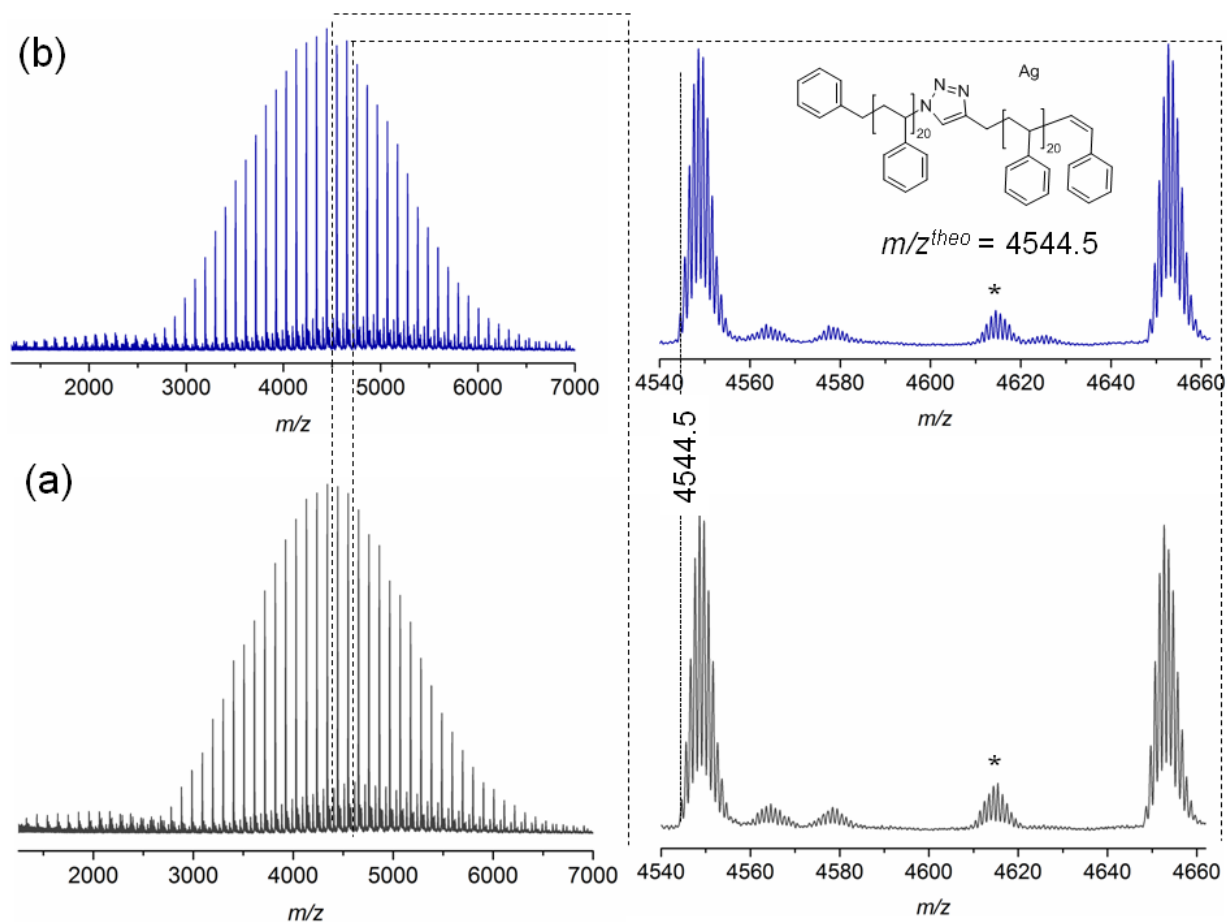


Figure 7. MALDI-MS spectra of polymer **11** before (a) and after (b) thermal treatment at 200 °C for 24 h in an argon atmosphere. *Refers to cationization of PS by $Ag_2NO_3^+$.

The stability of triazole mid-chain polystyrene is additionally confirmed by MALDI-MS analysis. As depicted in Figure 7, the mass spectra recorded for polystyrene **11** before and after thermal treatment do not exhibit any changes in both the width of the mass distributions nor the nature of the observed signals, resulting in completely identical spectra confirming a high thermal stability of the triazole group under inert atmosphere conditions.

The stability of the triazole unit after thermal treatment was additionally successfully evidenced by XPS. The N 1s spectrum of polystyrene **11** (refer to Figure S13 in the SI section) indicates two peaks, one at 400.1 eV (C-N-N-, C-N=N-), which can be attributed to the triazole unit^{36,37} and a second one at 401.6 eV which is probably due to a protonated species (C-HN⁺⁼). After thermal treatment of polystyrene **11**, the same spectral region can be evaluated (refer to Figure 10), indicating that the total amount of nitrogen is stable and exhibits quantities of close to 0.8 (± 0.1) at % before and 0.6 (± 0.1) at % after thermal treatment, evidencing the stability of the triazole unit. An assessment of the SEC, NMR and XPS data thus demonstrate that the triazole mid-chain functional linear polystyrene **11** does not suffer from degradation, thus indicating that the absence of the mid-chain functional position of the two ester units is critical for the stability of polystyrene **7a**.

Inspection of the ¹H NMR and MALDI-ToF spectra for polystyrene **1**, **2** and **3** clearly indicate that HBr elimination occurs during thermal treatment. As polystyrene **7a** indicates the formation lower and higher molecular species under thermal stress (refer to Figure 3), it is important to investigate if there is an additional effect on the decomposition of the ester group in polystyrene **7a** caused by the elimination of HBr at high temperatures during the thermal stress due to the acidic character of HBr. Thus, the bromine end group functionalities of the ATRP-made polymers were transformed to hydrogen end groups in the presence of tin hydride.³⁸ First of all, the bromine functionalities of polystyrene **3a** ($M_{n,SEC} = 6.1$ kDa, $D = 1.06$) and **3b** ($M_{n,SEC} = 39$ kDa, $D = 1.08$) were converted into hydrogen atoms to obtain polymers **12a** and **12b** in the presence Bu₃SnH, respectively. The low molecular weight of polystyrene **12a** was prepared for subsequent ¹H NMR analysis. The ¹H NMR spectrum (refer to Figure S14 in the SI section) of polystyrene **12a** indicates the disappearance of resonances associated with the CH-Br

proton between 4.30 and 4.60 ppm, clearly evidencing the successful conversion of bromine to hydrogen at the chain terminus. Polystyrene **12b** (for SEC analysis refer to Figure S15 in the SI section) was subjected to identical thermal degradation conditions (i.e. 200 °C for 24 h under inert atmosphere) as polystyrene **3a** and **3b**. Inspection of Figure S15 clearly indicates that thermal degradation of polystyrene **12b** in the absence of HBr is substantially less favorable after 24 h at 200 °C compared to polystyrenes **3a** and **3b**, showing a very small shoulder in the low molecular weight region due to Chugaev-type elimination, while the polystyrenes **3a** and **3b** display a new peak in the low molecular weight region (refer to Figure 5 for **3a** and refer to Figure S15 for **3b** in the SI section). These observations indicate that the HBr elimination during thermal degradation is the main effect on the ester degradation of the polystyrenes **3a** and **3b**.

It is mandatory to translate the above observation to the assessment of polystyrene **7a**. The bromine end group functionalities at the terminus of polystyrene **7a** was removed in the presence of the Bu_3SnH under identical reaction conditions as for polystyrenes **12a** and **12b** to obtain polymer **13a**, carrying no bromine functionality. Polystyrene **13a** was subjected to identical thermal degradation conditions (i.e. 200 °C for 24 h under inert atmosphere) as polystyrene **7a** prior to SEC analysis. The change in the molecular weight distribution as a function of time is depicted in Figure S16, indicating a small increasing D due to the formation of lower molecular weight species (Chugaev-type elimination of aliphatic esters). However, there is no indication of higher molecular weight species being formed, allowing the conclusion that HBr due to its acidic character has an additional effect the decomposition of the ester group of the polystyrene **7a**. Further, the formation of higher molecular weight species may also be related to the bromine end group functionalities, a hypothesis that is explored in detail below.

In addition, polystyrene **7b** was synthesized with low weight-average molecular weight for comparison with polystyrene **11** after thermal treatment. Polystyrene **7b** was subjected to the same thermal treatment as **11** prior to ^1H NMR (refer to Figure S17) and SEC (refer to Figure S18) analyses. The ^1H NMR spectrum of polystyrene **7b** indicates the disappearance of resonances associated with the ester protons as well as the protons adjacent to the triazole ring between 3.20 and 4.80 (refer to Figure S14 in the SI section), in agreement with ester degradation. Inspection of Figure S18 clearly indicates a decrease in the number-average molecular weight from $M_n = 3800$ Da to $M_n = 1900$ Da for polystyrene **7b** as a consequence of the appearance of a material with lower molecular weight. The mass spectra for polystyrenes **7b** before thermal treatment are depicted in Figure 8. For polystyrene **7b** before thermal treatment (Figure 8a), the recorded mass spectra present as main distribution the unsaturated species. After the thermal treatment of polystyrene **7b**, an inversion of the relative intensities of both distributions is observed. Since all mass spectra have been recorded under exactly the same experimental conditions, the change in the intensities shows the presence of a high intensity distribution of polystyrene with carboxylic end-groups (m/z 1962) at lower mass-to-charge ratio (Scheme 5), which unambiguously confirms the ester driven degradation as attested by SEC and ^1H NMR. These combined results (refer to Figure S11 and Figure S18 in the SI section) allow the conclusion that the presence of the HBr, which is formed during thermal treatment, enhances ester degradation. However, the ester degradation is faster for low molecular weight polystyrene **7b** than the high polymer weight polystyrene **7a** (refer to Figure 3 and Figure S18 in the SI section). This observation could be associated with the lower glass transition temperature as well as higher diffusion coefficient of the low molecular weight polystyrene **7b** compared to polystyrene **7a**. Thus, polystyrene **7c** ($M_n = 33.7$ kDa, $D = 1.09$) was synthesized via ARGET

ATRP – featuring a higher molecular weight than polystyrene **7b** – thus leading to less degradation than polystyrene **7b**.

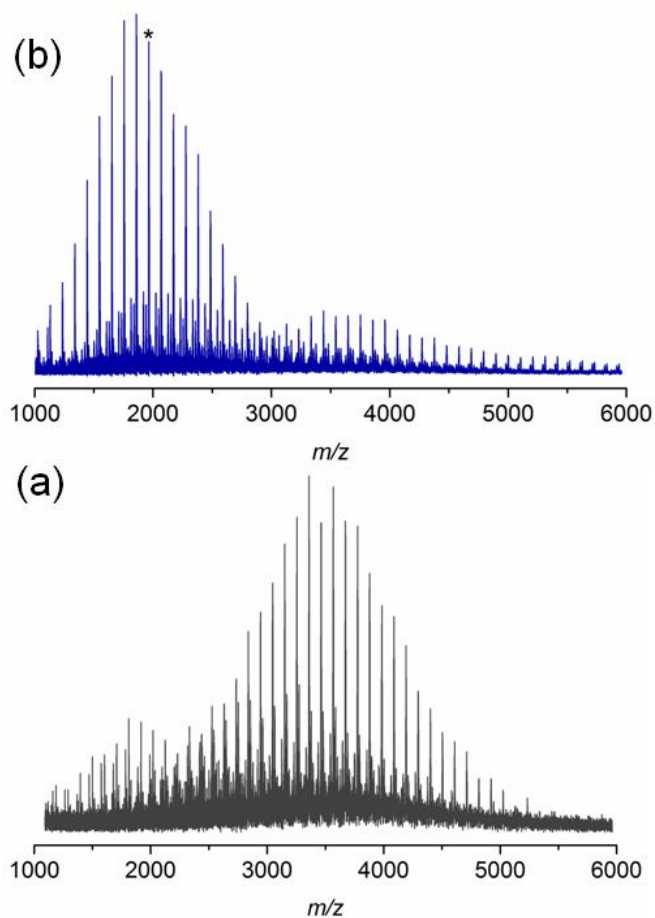
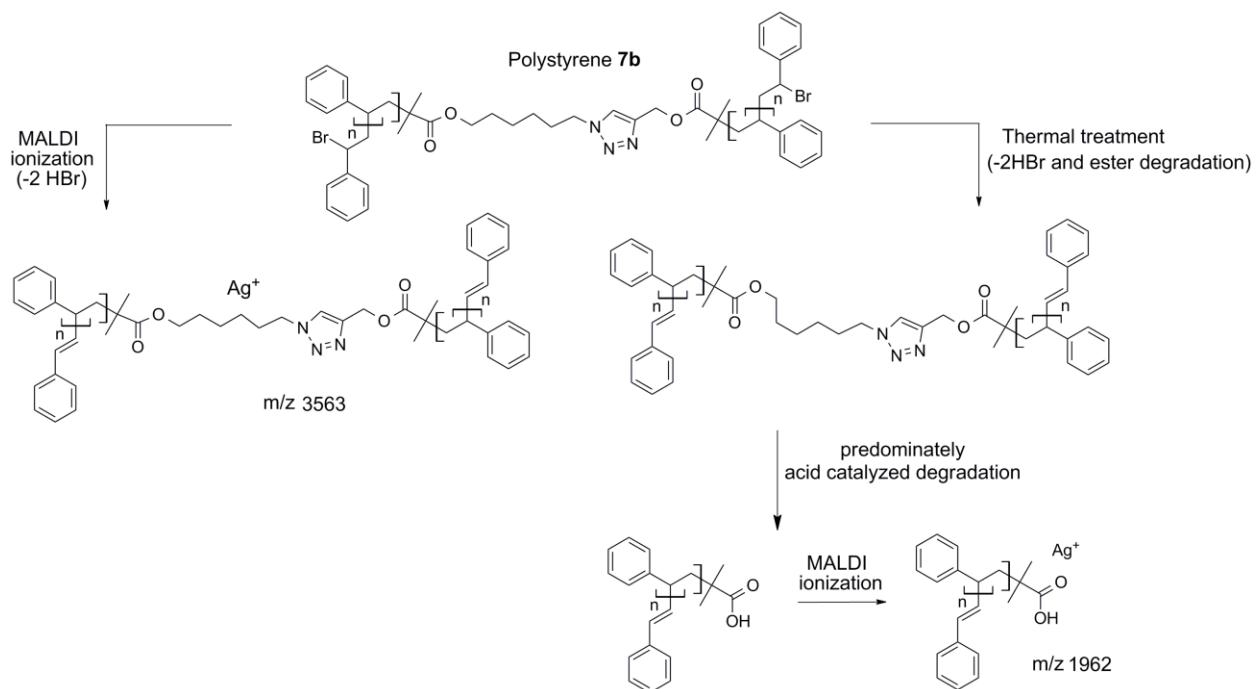


Figure 8. MALDI-MS spectra of polymer **7b** before (a) and after (b) thermal treatment at 200 °C for 24 h in an argon atmosphere. After thermal treatment, (b), the presence of polystyrenes with carboxylic end-groups (the peak marked with an asterisk is at m/z 1962) at lower mass-to-charge ratios confirm the ester driven degradation process (Scheme 5).



Scheme 5. Depiction of the mechanistic pathway to the structures observed by MALDI-MS analysis of polystyrene **7b** (a) before and (b) after thermal treatment (200 °C, 24 h).

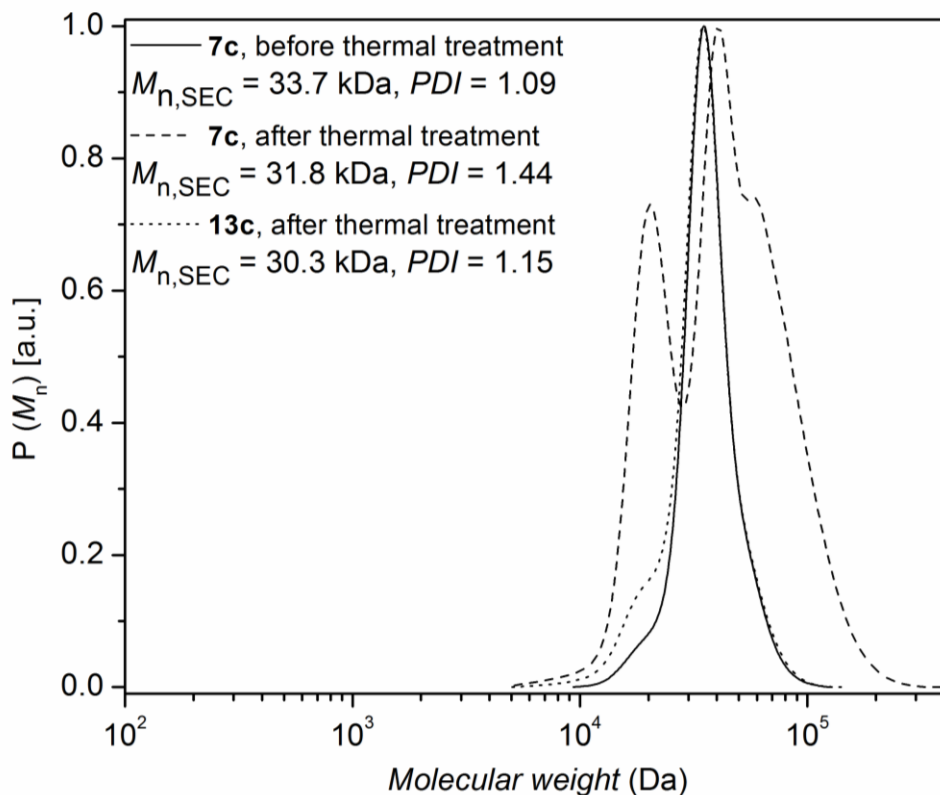


Figure 9. SEC traces of polystyrene **7c** before thermal treatment as well as polystyrene **7c** and polystyrene **13c** after thermal treatment at 200 °C for 24 h in an argon atmosphere.

The same thermal conditions as for polystyrene **7a** and **7b** were applied to polystyrene **7c**. The change in the molecular weight distribution of polystyrene **7c** as a function of time is depicted in Figure 9, indicating an increasing D , congruent with the formation of lower molecular weight species resulting from ester decomposition.³⁵ The bromine functionalities of the polystyrene **7c** ($M_{n,SEC} = 33.7$ kDa, $D = 1.09$) were subsequently converted to hydrogen atoms to obtain polystyrene **13c**, which was subjected to identical thermal treatment conditions as polystyrene **7c**. The change in the molecular weight distribution of polystyrene **13c** is depicted in Figure 9, indicating a slight increase in D due to the formation of lower molecular weight species with time (Chugaev-type elimination of aliphatic esters). However, there is no indication

for the formation of higher molecular weight species and the ester degradation is slow in the absence of HBr. Importantly, in order to investigate the effect of HBr elimination on the ester degradation, polystyrene **7a** in the presence of decyl bromide – to increase the HBr content – was subjected to thermal treatment at 200 °C for 24 h under argon atmosphere. The change in the molecular weight distribution is depicted in Figure S19 in the SI section, indicating that ester groups present in polystyrene **7a** completely degrade in the presence of excess decyl bromide – to approximately half their initial M_n – at 200°C within 24 h. This observation underpins the effect of HBr elimination on the decomposition of the ester group in polystyrene **7a**.

These observations so far demonstrate that (i) the polystyrenes **7a** and **7c** – containing ester functionalites, bromine termini as well as a triazole units – form higher and lower molecular weight species upon thermal stress (refer to Figure 3 and Figure 9), (ii) there are only lower molecular weight species formed in the presence of ester and bromine end functional polystyrenes **3a** and **3b** (refer to Figure 5 and Figure S15 in the SI section), (iii) when the bromine termini of polystyrene **3b** are removed (**12b**), very small amounts of the low molecular weight species are observed (refer to Figure S15 in the SI section) due to the Chugaev-type elimination of aliphatic esters, (iv) in the absence of the bromine termini and in the presence of ester and triazole units, higher molecular weight species are no longer formed and a very small amount of lower molecular species is formed (polystyrene **13a** and **13c**, refer to Figure 9, Figure S16 and Figure S20 in the SI section) due to the Chugaev-type elimination of aliphatic esters. These observations suggest that there exists a reaction between the bromine end functionalities and the triazole unit. Interestingly, Drockenmuller and co-workers have proposed a straightforward synthetic route to a new class of ion conducting materials possessing 1,2,3-triazolium charged units via an efficient 1,2,3-triazole quaternization.^{39,40} The molecular weight

of polystyrene **7a** is too high for a meaningful end group analysis. Thus, polystyrene **7b** was treated with a 20-fold excess of decyl bromide at 100 °C for 16 h in DMF to obtain polystyrene **14**. After purification, the ¹H NMR spectrum of polystyrene **14** clearly indicates the formation of the triazolium salt in the presence of decyl bromide. Further, the bromine atoms of polystyrene **14** are eliminated from the structure generating unsaturated species in solution (refer to Figure 10). The ¹H NMR spectrum indicates that the characteristic resonances associated with the CH₂ of the decyl group adjacent to the triazole ring at 4.88 ppm as well as new resonances related to CH in the triazole ring at 10.09 ppm emerged, evidencing the successful ligation between the triazole ring and the alkyl group in excellent agreement with previous observation in the literature^{39,40} (refer to Figure 9). The SEC analysis of polystyrene **14** indicates that there is no change in the number-average molecular weight after treatment with decyl bromide (refer to Figure S20 in the SI section). MALDI-ToF spectra for polystyrene **14** clearly indicate the formation of the triazolium salt (refer to Figure S21 in the SI section).

Polystyrene **14** was subsequently subjected to thermal treatment at 200 °C for 24 h under argon atmosphere (refer to Figure S20 in the SI section). Inspection of Figure S20 clearly indicates that thermal degradation of the ester group of polystyrene **14** in the absence of HBr is substantially less favorable after 24 h at 200 °C compared to polystyrenes **7b** in Figure S18 in the SI section, showing a very small shoulder in the low molecular weight region due to the Chugaev-type elimination of aliphatic esters. The polystyrenes **7b** display a new peak in the low molecular weight region.

These observations (refer to Figure 3, Figure 8 and Figure 10) support the hypothesis that the formation of higher molecular weight species during thermal treatment of polystyrene **7a** and **7c** is due to the formation of triazolium salts.

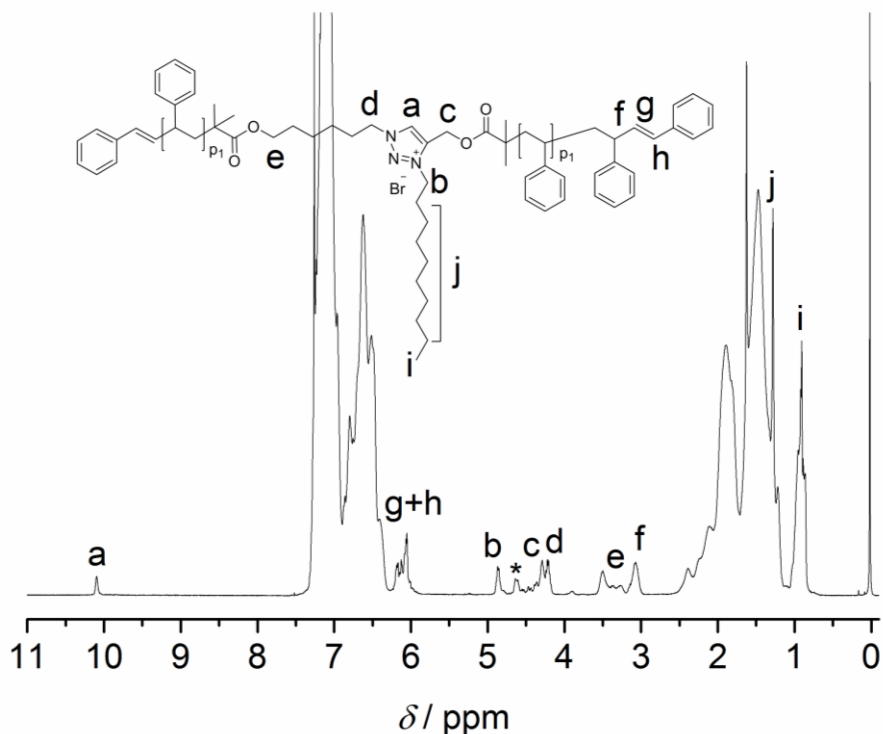


Figure 10. ^1H NMR spectra of polystyrene (**7b**) recorded in CDCl_3 at ambient temperature after treatment with decyl bromide at $100\text{ }^\circ\text{C}$ in DMF for 16 h in an argon atmosphere. The resonance marked with an asterisk is due to remaining bromine end functional polystyrene **7b**.

Rheological Assessment and Extrusion Conditions

In a subsequent step – after establishing the level of stability of the individual functional groups at elevated temperatures – the melt rheological and extrusion behavior of polystyrene **7a** featuring all functional groups as well as polystyrene **13a** carrying ester and triazole functional groups was investigated.

The polymers may undergo degradation caused by temperature under inert atmosphere as well as additional mechanical stresses during processing. All dynamic measurements were carried out within the linear response domain adjusting the strain amplitude accordingly. The viscoelastic properties of the polymers were measured in small-amplitude oscillatory shear

(LAOS) flow as a function of time at certain temperatures and strain amplitude with a constant frequency.^{41,42} The rheological properties can be monitored continuously as a function of the time (e.g. several seconds time resolution) and therefore the degradation process of the samples is assessed by rheological properties especially via the zero shear viscosity, $\eta_0 = \lim_{\dot{\gamma} \rightarrow 0} \eta(\dot{\gamma}) = \lim_{\omega \rightarrow 0} |\eta^*(\omega)|$, throughout the degradation process applying the Cox-Merz rule.^{20,21} This assumption is reasonable as we investigate linear, monodisperse homopolymers. The following section will detail the results with respect to the zero shear viscosity and in comparison with the weight-average molecular weight obtained by SEC after applying a thermomechanical stress with the weight-average molecular weight (and distribution) of polystyrene **7a**. The absolute value of the complex viscosities as a function of time at a temperature of 180 °C at a frequency of $\omega_1/2\pi = 0.05$ Hz and 15% strain amplitude for the polystyrene **7a** are used to determine the zero shear viscosity, $\eta_0 = \lim_{\dot{\gamma} \rightarrow 0} \eta(\dot{\gamma}) = \lim_{\omega \rightarrow 0} |\eta^*(\omega)|$, assuming the validity of the Cox-Merz rule. These data are depicted in Figure 11. Dynamic frequency sweep test depicted in Figure S22 shows that the zero shear viscosity, $\eta_0 = \lim_{\omega \rightarrow 0} |\eta^*|$, has been reached for shear frequencies below 0.1 Hz for stable polystyrenes (e.g. after an 24 hour under time sweep test at 180 °C where maximum zero shear viscosity was reached, refer to Figure 11). Inspection of Figure 11 indicates that the zero shear viscosity of polystyrene **7a** increases from the initial value of 10 kPa s up to 17 kPa s during three hours. After this period, the zero shear viscosity was constant during seven hours and subsequently decreases with increasing time at elevated temperatures. It is worth noting that for polystyrene with M_w larger than the critical molecular weight M_c ($\approx 3M_e$; M_e ca. 18 kDa for polystyrene), reptation theory describes the dependence of the zero shear viscosity on weight-average molecular weight via a

cubic power law. The zero shear viscosity of linear polystyrene was studied earlier⁴³ at the reference temperature $T_{\text{ref}} = 170$ °C, $\eta_{0,\text{Linear PS}} = 8.8 \times 10^{-14} M_w^{3.4}$, and the WLF shift factor, $\log a_T = -5.47(T - 170) / (119 + (T - 170))$, where T is given in Celsius. Using this shift factor, the zero shear viscosity for linear polystyrene was re-calculated at $T = 180$ °C:

$$\eta_{0,\text{Linear PS}} = 3.31 \times 10^{-14} M_w^{3.4} ; T = 180 \text{ °C} \quad (1)$$

With respect to the experimental values of zero shear viscosity of polystyrene **7a** in Figure 11 and equation (1), the weight-average molecular weight of this polymer is predicted and plotted in Figure 11 on the left y-axis. The weight-average molecular weight evolution of polystyrene **7a** (as recorded via time dependent SEC, refer to Figure 3) is plotted in Figure 11 (open circles), clearly indicating that the SEC derived weight-average molecular weights (M_w) are in agreement with the values predicted from rheological data (specially the zero shear viscosity) and reptation theory. It should be noted that thermal degradation decreases the number-average molecular weight, M_n , while increasing the polydispersity and subsequently the weight-average molecular weight, M_w , to some extent. The observed increase of the zero shear viscosity during the thermal degradation reflects to M_w rather than M_n .

After applying both thermal and mechanical stress (in the linear regime) at a temperature of 180 °C for 24 h at a frequency of $\omega_1/2\pi = 0.05$ Hz and 15% strain amplitude for the polystyrene **7a**, the molecular weight of the polystyrene **7a** was determined by SEC (refer to Figure S23 in the SI section). The SEC analysis also revealed that the molecular weight of polystyrene **7a** has changed. While weight-average molecular weight of the polystyrene **7a** under thermomechanical stress decrease from $M_w = 148$ kDa to $M_w = 142$ kDa, the number-average molecular weight of the same polystyrene reduce from $M_n = 124$ kDa to $M_n = 87$ kDa. The change in number-average molecular weight, M_n , observed for polystyrene **7a** is higher than the

change observed for the weight-average molecular weight, M_w . On the other hand, the SEC data obtained via the time resolved SEC analysis for polystyrene **7a** subjected to only thermal stress for 24 h, reflects an increase in weight-average molecular weight from $M_w = 148$ kDa to $M_w = 161$ kDa (refer to Figure S23 in the SI section) and a reduction in number-average molecular weight from $M_n = 124$ kDa to $M_n = 109$ kDa. Thus, combined mechanical and thermal stress has a distinct effect on the cleavage and degradation process of polystyrene **7a** compared to thermal stress alone perhaps due to increased convection in the sample. In other words, the degradation process becomes prominent during the rheological characterization of polystyrene **7a**.

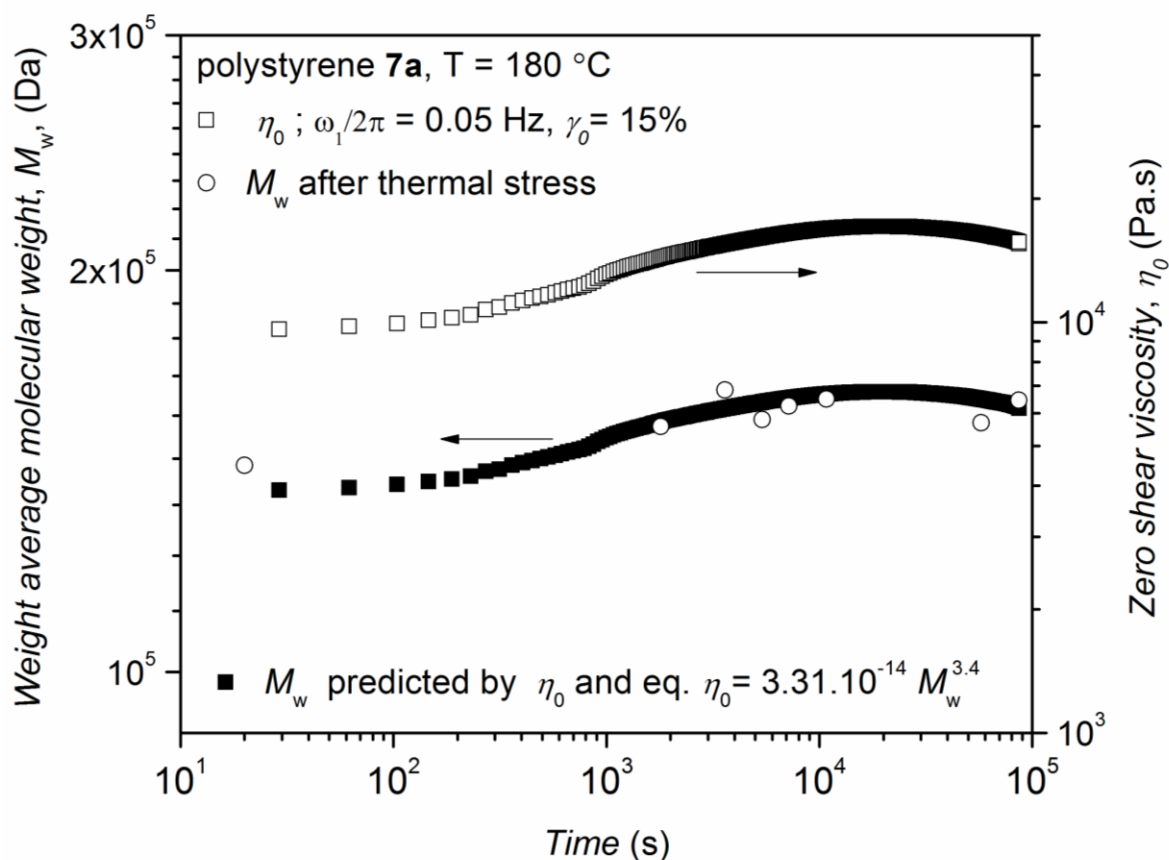


Figure 11. Time dependence of the experimental zero shear viscosity of the polystyrene **7a** (right y-axis) and weight-average molecular weight of the polymer **7a** deduced from time dependent SEC (left y-axis) along with the weight-average molecular weight based on the

experimental zero shear viscosity and eq. (1). The higher time resolution and lower standard deviation of the rheological assessment can be seen while SEC allows analysis of the full molecular weight distribution.

In order to investigate the effect of HBr elimination on the ester degradation, the zero shear viscosity polystyrene **13a** as a function of time for 24 h at a frequency of $\omega_1/2\pi = 0.05$ Hz and 15% strain amplitude was measured (refer to Figure S24 in the SI section). Inspection of Figure S24 indicates that the zero shear viscosity of polymer **13a** is constant up to 60 minutes and subsequently slowly decreases with increasing time at elevated temperatures in the linear regime due to degradation and a slight reduction of molecular weight induced by thermomechanical stress. Further inspection of Figure S24 indicates that there is no increase in the zero shear viscosity with increasing time at elevated temperatures, whereas the same rheological parameter for polystyrene **7a** demonstrated an increase in the zero shear viscosity (refer to Figure 11). The results obtained are in qualitative agreement with the studies invoking thermal stress alone for polystyrene **13a**. After applying thermomechanical stress to polystyrene **13a** in the above experiment, SEC analysis revealed that the molecular weight distributions of polystyrene **13a** had experienced a slight change. The molecular weight reduction observed during thermomechanical stress at elevated temperatures can be compared to the reduction in molecular weight observed in solely pure thermal degradation experiments for polystyrene **13a** (refer to Figure S25 in the SI section). The relative values for the number-average molecular weight based on SEC before/after thermal stress were found to be close to 118.1 vs. 112.3 kDa for polystyrene **13a**. Comparing the number-average molecular weight obtained for polystyrene **13a**, it appears that the rheology experiment had no an additional effect on the degradation behavior due to thermomechanical stress in the absence of bromine end groups.

Polymer processing allows shaping and manufacturing polymers in powder or pellet form. The extrusion process is a continuous shaping of a polymer in the melt through the orifice of a die and the subsequent solidification into a product. To mimic the extrusion process of the polystyrene **7a** containing ester, triazole and bromine functionalities, a 10 minute residence time in the extrusion barrel – consistent with the mixing average residence time common in extrusion processes – was selected. However, feeding of the polymers took close to 10 minutes, therefore the total residence time is close to 20 minutes at 200 °C. The change in molar mass after extrusion is a sensor for the combined effects of thermal and mechanical degradation on the polymeric material, due to the orientation and stretch of the polymer chains that can influence their stability. The molecular weight reduction observed during extrusion can be compared to the reduction in molecular weight observed in pure thermal degradation experiments for polystyrene **7a**. The change in the number-average molecular weight of polystyrene **7a** after extrusion was determined via SEC (refer Figure 12). The relative values for the number-average molecular weight based on SEC before/after extrusion were found to be close to 124.6 kDa vs. 108.6 kDa corresponding to a 12% decrease for polystyrene **7a**, respectively. In our previous study,¹⁷ 10% reduction in molecular weight after the extrusion at 200°C after 20 min was observed for anionically prepared non-functional linear polystyrene. Comparing the number-average molecular weight obtained by SEC before and after extrusion, a slight reduction in molecular weight was observed. It appears that the extrusion process for mid-chain triazole functionalized linear polystyrene with mid chain ester and end chain bromine functionalities had no significant effect on the degradation behavior due to additional mechanical stress at short times.

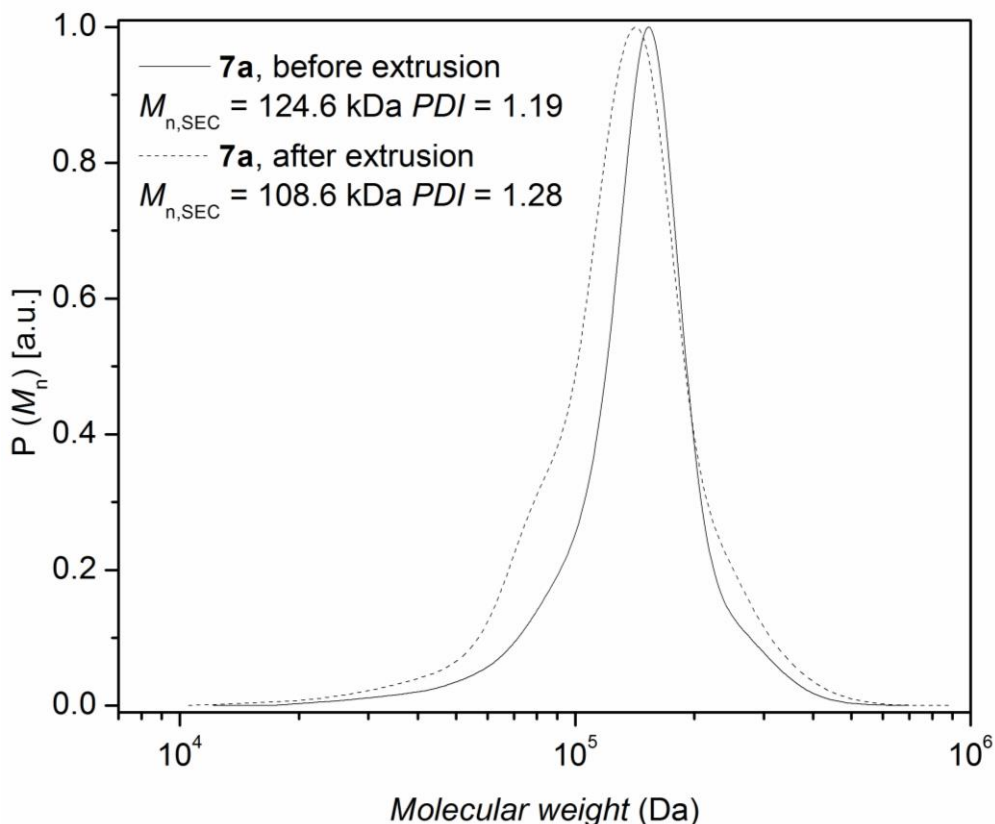


Figure 12. Comparison of the molecular weight distribution of polystyrene **7a** before and after extrusion in a twin screw extruder at 200 °C with total residence time of 20 min.

CONCLUSIONS

In summary, the stability of living/controlled polystyrenes generated by activators regenerated by electron transfer (ARGET) atom transfer radical polymerization (ATRP) with ester and triazole mid-chain functionalities and a secondary bromine chain-end functionality was investigated under thermal and thermomechanical stress in an inert atmosphere at elevated temperatures. The thermally treated linear polystyrene containing the above functions (**7a**) were analyzed by size exclusion chromatography as a function of their exposure time to elevated temperatures (e.g. 200 °C) indicating a degradation of the functional polystyrene. The stability of

these three functional groups was systematically investigated under nitrogen atmosphere at elevated temperatures to identify the cleavage points of polystyrene **7a**. Linear polymers having either a secondary alkyl halide (**1** or **2**), ester group (**3a** and **3b**) or triazole moieties (**11**) were prepared as low molecular weight reference polymers and subsequently exposed to elevated temperatures under inert atmosphere. The thermally treated polystyrenes at elevated temperature were evaluated by SEC, ^1H NMR and MALDI-MS demonstrating the cleavage of the ester group as well as the quaternization of the triazole unit in the presence of the bromine end groups of the ATRP-made polymers. Thus, any high temperature processing or storage of polymers – or at least polystyrenes – prepared via ATRP should avoid the mid-chain presence of any ester groups and triazole unit. When the bromine end groups of the ATRP-made polymers are removed before thermal/thermomechanical treatment, ester degradation almost ceases. Importantly, the chain ends of the ATRP polymers can undergo a quaternization reaction with the triazole units present in the polymer chain, leading to the formation of higher molecular weight material. An in-depth rheological assessment revealed that the number-average molecular weight, M_n , of the mid-chain functional linear polymer decreases under conditions of oscillatory shear at $180\text{ }^\circ\text{C}$ with $\omega_1/2\pi = 0.05\text{ Hz}$ and $\gamma_0 = 15\%$ strain amplitude, while the polydispersity and the weight-average molecular weight, M_w , generally increases. These findings are in agreement with the on-line monitoring of the zero shear viscosity under the above oscillatory shear conditions. SEC analysis revealed that the number-average molecular weight of polystyrene **7a** was reduced by 30% under thermomechanical stress during rheological characterization of polystyrene **7a**, indicating an additional effect on the degradation behavior, while polystyrene **7a** shows 10% reduction in number-average molecular weight with thermal stress alone. Moreover, an assessment of polystyrene **13a** carrying no bromine functionalities indicates that there is no increase in the zero shear viscosity with time under the above oscillatory shear conditions. In addition, SEC traces

recorded after extrusion for 20 minutes under an inert atmosphere at 200 °C indicate that the number-average molecular weight of the linear polystyrene **7a** decreases by 12%, while the chain-end functional or non-functional linear polystyrenes indicate a reduction by close to 10% in number-average molecular weight, suggesting that mechanical stress has slight effect on the degradation of functional linear polystyrene **7a** during the extrusion process.

Table 2 collates the identified behavior after thermal insult for all studied polymer systems.

Table 2. The number average-molecular weight of polystyrenes before and after thermal treatment. Plus indicates the presence, minus the absence of the functional group. Note that for fully judging the molecular weight after thermal insult, the respective full MWDs must be inspected.

Polymer	Ester	Triazole	Bromine	$M_n^{a,b}$	$\mathcal{D}^{a,b}$	$M_n^{a,c}$	$\mathcal{D}^{a,c}$
1	-	-	+	2	1.06	2	1.06
3a	+	-	+	6.5	1.06	4.2	1.20
3b	+	-	+	39	1.08	28.1	1.18
7a	+	+	+	125	1.19	95.1	1.63
7b	+	+	+	3.8	1.07	1.9	1.23
7c	+	+	+	33.7	1.09	31.8	1.44
11	-	+	-	4.4	1.08	4.3	1.08
12b	+	-	-	38.5	1.06	34.1	1.13
13a	+	+	-	118.1	1.19	112.3	1.23
13c	+	+	-	32.5	1.09	30.3	1.15

^a Determined via RI detection SEC using linear PS standards. ^b before thermal treatment; ^c after thermal treatment at 200 °C for 24 h under inert atmosphere. The molecular weight values are given as kDa.

In summary, it is strongly recommended that ATRP polymers based on initiators with ester linkages in critical positions (as is often the case in those available commercially) and/or triazole units anywhere in the molecular structure, are not subjected to any thermal stress or processing, unless the bromine termini are removed.

Supporting Information Available: ^1H NMR spectra of the compounds **3a**, **6**, **8**, **9**, **10**, **11**, **12a**; ^{13}C NMR spectrum of the compound **6**; evolution of ATR-IR spectra of the polymers **8**, **10**, and **11**; SEC traces of polymer **7a** after thermal treatment at 200 °C in an argon atmosphere as a function of time; SEC traces of polystyrene **3b**, **7b**, and **12b** after thermal treatment at 200 °C in an argon atmosphere for 24 h, ^1H NMR spectra of the polymers before and after thermal treatment **1**, **2**, **3**, **7b**, **11**; MALDI-MS spectra of polystyrene **1** before and after thermal treatment at 200 °C for 24 h in an argon atmosphere; the storage (G') and loss modulus (G'') as a function of frequency at 180 °C for polystyrene **7a** and **13a**, supporting SEC data for the rheological experiments; SEC traces and MALDI-MS spectrum of polystyrene **14**.

ACKNOWLEDGMENTS

C.B.-K and M.W. gratefully acknowledge financial support from the German Research Council (DFG). The authors acknowledge additional funding for the current project from the Karlsruhe Institute of Technology (KIT). P.G. thanks the financial support from the Wallonia Region, the European Commission (FSE, FEDER), the National Fund for Scientific Research (F.R.S.-FNRS), and the Belgian Federal Science Policy Office (PAI 6/27). O.A. thanks Dr. Eva Blasco (KIT), Andrea Hufendiek (KIT) and Ralf A. A. Bovee (Eindhoven Technical University, TU/e) for helpful discussions.

REFERENCES AND NOTES

- (1) H. C. Kolb, M. G. Finn, K. B. Sharpless, *Angew. Chem. Int. Ed.*, 2001, **40**, 2004–2021.

- (2) V. V. Rostovtsev, L. G. Green, V. V. Fokin, K. B. Sharpless, *Angew. Chem. Int. Ed.*, 2002, **41**, 2596-2599.
- (3) C. Barner-Kowollik, F. E. Du Prez, P. Espeel, C. J. Hawker, T. Junkers, H. Schlaad, W. V. Camp, *Angew. Chem. Int. Ed.*, 2011, **50**, 60–62.
- (4) W. A. Braunecker, K. Matyjaszewski, *Prog. Polym. Sci.*, 2007, **32**, 93–146.
- (5) P. L. Golas, K. Matyjaszewski, *Chem. Soc. Rev.*, 2010, **39**, 1338–1354.
- (6) J.-F. Lutz, H. G. Boerner, K. Weichenhan, *Macromolecules*, 2006, **39**, 6376–6383.
- (7) J. A. Opsteen, J. C. M. van Hest, *Chem. Commun.*, 2005, 57–59.
- (8) O. Altintas, G. Hizal, U. Tunca, *J. Polym. Sci., Part A: Polym. Chem.*, 2006, **44**, 5699–5707.
- (9) J. A. Johnson, D. R. Lewis, D. D. Diaz, M. G. Finn, J. T. Koberstein, N. J. Turro, *J. Am. Chem. Soc.*, 2006, **128**, 6564–6565.
- (10) M. Malkoch, K. Schleicher, E. Drockenmuller, C. J. Hawker, T. P. Russell, P. Wu, V. V. Fokin, *Macromolecules*, 2005, **38**, 3663–3678.
- (11) K. Matyjaszewski, J. Xia, *Chem. Rev.*, 2001, **101**, 2921–2990.
- (12) R. T. A. Mayadunne, E. Rizzardo, J. Chiefari, Y. K. Chong, G. Moad, S. H. Thang, *Macromolecules*, 1999, **32**, 6977–6980; *Handbook of RAFT-Polymerization*; Barner-Kowollik, C., Ed.; Wiley-VCH: Weinheim, Germany, 2008.
- (13) C. J. Hawker, A. W. Bosman, E. Harth, *Chem. Rev.*, 2001, **101**, 3661–3688.
- (14) N. V. Tsarevsky, K. Matyjaszewski, *Chem. Rev.*, 2007, **107**, 2270–2299.
- (15) O. Altintas, A. P. Vogt, C. Barner-Kowollik, U. Tunca, *U. Polym. Chem.*, 2012, **3**, 34–45.

- (16) R. K. Iha, K. L. Wooley, A. M. Nyström, D. J. Burke, M. J. Kade, C. J. Hawker, *Chem. Rev.*, 2009, **109**, 5620–5686.
- (17) O. Altintas, K. Riazi, R. Lee, C. Y. Lin, M. L. Coote, M. Wilhelm, C. Barner-Kowollik, *Macromolecules*, 2013, **46**, 8079–8091.
- (18) O. Altintas, M. Abbasi, K. Riazi, A. S. Goldmann, N. Dingenouts, M. Wilhelm, C. Barner-Kowollik, *Polym. Chem.*, 2014, **5**, 5009-5019.
- (19) *Scaling Concepts in Polymer Physics*, P. G. de Gennes, Cornell University Press, London, UK, 1979.
- (20) *Introduction to Polymer Rheology*, M. T. Shaw, John Wiley & Sons, New Jersey, USA, 2012.
- (21) *The Structure and Rheology of Complex Fluids*, R. G. Larson, Oxford University Press, New York, USA, 1999.
- (22) *Rheology: Principles, Measurements, and Applications*, C. W. Macosko, Wiley-VCH, Weinheim, Germany, 1994.
- (23) E. H. H. Wong, O. Altintas, M. H. Stenzel, C. Barner-Kowollik, T. Junkers, *Chem. Commun.*, 2011, **47**, 5491–5493
- (24) W. Lin, Q. Fu, Y. Zhang, J. Huang, *Macromolecules*, 2008, **41**, 4127–4135.
- (25) K. Matyjaszewski, *Macromolecules*, 2012, **45**, 4015–4039.
- (26) T. Gruendling, S. Weidner, J. Falkenhagen, C. Barner-Kowollik, *Polym. Chem.*, 2010, **1**, 599–617.
- (27) G. Luo, I. Marginean, A. Vertes, *Anal. Chem.*, 2002, **74**, 6185–6190.

- (28) X. Jiang, P. J. Schoenmakers, J. L. J. van Dongen, X. Lou, V. Lima, J. Brokken-Zijp, *Anal. Chem.* 2004, **75**, 5517–5524.
- (29) C. Ladavière, P. Lacroix-Desmazes, F. Delolme, *Macromolecules*, 2009, **42**, 70–84.
- (30) J. De Winter, M. Vachaudéz, O. Coulembier, P. Dubois, R. Flammang, P. Gerbaux, P. *E-Polymers*, 2010, **103**, 1–10.
- (31) J. De Winter, V. Lemaur, P. Marsal, O. Coulembier, J. Cornil, P. Dubois, P. Gerbaux, *J. Am. Soc. Mass Spectrom.*, 2010, **21**, 1159–1168.
- (32) J. De Winter, O. Coulembier, P. Dubois, P. Gerbaux, *Inter. J. Mass Spectrom.*, 2011, **308**, 11–17.
- (33) C. D. Hurda, F. H. Blunck, *J. Am. Chem. Soc.*, 1938, **60**, 2419–2425.
- (34) G. L. O'Connor, H. R. Nace, *J. Am. Chem. Soc.*, 1953, **75**, 2118–2123.
- (35) H. A. Pohl, *J. Am. Chem. Soc.*, 1951, **73**, 5660–5661.
- (36) F. Bentiss, M. Traisnel, L. Gengembre, M. Lagrene, *Appl. Surf. Sci.*, 1999, **152**, 237–249.
- (37) E. Blasco, M. Piñol, L. Oriol, B. V. K. J. Schmidt, A. Welle, V. Trouillet, M. Bruns, C. Barner-Kowollik, *Adv. Funct. Mater.*, 2013, **23**, 4011–4019.
- (38) V. Coessens, K. Matyjaszewski, *Macromol. Rapid Commun.*, 1999, **20**, 66–70.
- (39) P. Dimitrov-Raytchev, S. Beghdadi, A. Serghei, E. Drockenmuller, *J. Polym. Sci. Polym. Chem.*, 2013, **51**, 34–38.
- (40) M. M. Obadia, B. P. Mudraboyina, A. Serghei, T. N. T. Phan, D. Gimes, E. Drockenmuller, *ACS Macro Lett.*, 2014, **3**, 658–662.

- (41) M. Kempf, D. Ahirwal, M. Cziep, M. Wilhelm, *Macromolecules*, 2013, **46**, 4978–4994.
- (42) K. Hyun, M. Wilhelm, *Macromolecules*, 2009, **42**, 411–422.
- (43) J. Hepperle, H. Muenstedt, P. K. Haug, C. D. Eisenbach, *Rheol. Acta*, 2005, **45**, 151–163.

ATRP-based Polymers with Modular Ligation Points under Thermal and Thermomechanical Stress

Ozcan Altintas, Thomas Josse, Mahdi Abbasi, Julien De Winter, Vanessa Trouillet, Pascal Gerbaux, Manfred Wilhelm* and Christopher Barner-Kowollik*

